(2)

AD-A265 704

ATION PAGE

Form Approved
OMB No. 0704-0188

1. AGENCY USE ONLY (Leave blank)	2. REPORT DATE	3. REPORT TYPE AND DATES COVERED
		Final Report 15 Dec 88 - 15 Dec 92

4. TITLE AND SUBTITLE
Ultrasonic Wave Interaction with Advanced Complex Materials for Nondestructive Evaluation Applications

5. FUNDING NUMBERS
AFOSR-89-0177

6. AUTHOR(S)
Professor Adnan H. Nayfeh

7. PERFORMING ORGANIZATION NAME(S) AND ADDRESS(ES)
Department of Aerospace Engineering and Engineering Mechanics

8. PERFORMING ORGANIZATION REPORT NUMBER
AFOSR-TR

9. SPONSORING / MONITORING AGENCY NAME(S) AND ADDRESS(ES)
AFOSR/NE
110 Duncan Avenue Suite B115
Bolling AFB DC 20332-0001

HAROLD WEINSTOCK

10. SPONSORING / MONITORING AGENCY REPORT NUMBER
2306/A3

DTIC
ELECTE
JUN 14 1993
S C D

11. SUPPLEMENTARY NOTES

12a. DISTRIBUTION / AVAILABILITY STATEMENT
UNLIMITED

12b. DISTRIBUTION CODE

13. ABSTRACT (Maximum 200 words) During the period of the grant we continued our modeling and analysis of the mechanical behavior of complex composite materials. We have developed analytical and numerical modeling techniques of the influence of general composite laminate orientation on the ultrasonic behavior of anistropic plates and substrates. In the second phase we introduced pizoelectric effects into our modeling. In the final phase we studied the dynamic response of the layered composite to transient loadings in the form of time dependent source loads. Complete documentation of the results of the first two phases were submitted to the AFOSR in the form of yearly reports. Since these reports contained completed items which also appeared in the literature as archival publications, we need not rereport them here. Results for the recently completed works have also been prepared for journal publication. Description of these works are included here in details

93-13119

14. SUBJECT TERMS

16. PRICE CODE

17. SECURITY CLASSIFICATION OF REPORT	18. SECURITY CLASSIFICATION OF THIS PAGE	19. SECURITY CLASSIFICATION OF ABSTRACT	20. LIMITATION OF ABSTRACT
UNCLASSIFIED	UNCLASSIFIED	UNCLASSIFIED	UNLIMITED

FINAL TECHNICAL REPORT

Grant: AFOSR-89-0177

Period: December 15, 1988 - December 15, 1992

Ultrasonic Wave Interaction with Advanced Complex Materials for Nondestructive Evaluation Applications

Adnan H. Nayfeh

Department of Aerospace Engineering and Engineering Mechanics
University of Cincinnati
Cincinnati, OH 45221

During the period of the grant we continued our modeling and analysis of the mechanical behavior of complex composite materials. We have developed analytical and numerical modeling techniques of the influence of general composite laminate orientation on the ultrasonic behavior of anisotropic plates and substrates. In the second phase we introduced piezoelectric effects into our modeling. In the final phase we studied the dynamic response of the layered composite to transient loadings in the form of time dependent source loads. Complete documentation of the results of the first two phases were submitted to the AFOSR in the form of yearly reports. Since these reports contained completed items which also appeared in the literature as archival publications, we need not rereport them here. Results for the recently completed works have also been prepared for journal publication. Description of these works are included here in details.

Chapter 1

WAVE PROPAGATION IN ANISOTROPIC MEDIA DUE TO INTERNAL HARMONIC LINE LOADS

1.1 Introduction

Plane harmonic wave interaction with homogeneous elastic anisotropic media, in general, and with layered anisotropic media, in particular, have been extensively investigated in the past decade or so. This advancement has been prompted, at least from a mechanics point of view, by the increased use of advanced composite materials in many structural applications. Being both anisotropic and dispersive, composite materials required indepth understanding of their mechanical behavior. The list of relevant literature is rather long and we thus refer the reader to selective recent works for further representative references [1-6]. Some of the difficulties inherent in the treatment of wave propagation in anisotropic media can be illustrated by considering slowness wave surface methods for infinite media [1,7-9] (Synge, 1957; Fedorov, 1968; Mus-

grave, 1970). According to this analysis, the slowness surface of an isotropic material consists of two concentric spherical sheets, an inner one representing the longitudinal wave mode and an outer one representing the two degenerate transverse modes. In the anisotropic case, we find there are three general wave surfaces, one for the so-called quasi-longitudinal wave and two nondegenerate sheets for the quasi-transverse waves. Moreover, the surfaces will no longer be spherical in shape but will reflect the elastic symmetry or assymetry of the material. Perhaps the most severe consequence of elastic anisotropy in infinite media is the loss of pure wave modes for general propagation directions. This fact also implies that the direction of energy flow (i.e., group velocity) does not generally coincide with the wave vector, or wavefront normal. Clearly, uncoupled pure potentials (such as are found in the isotropic case) are much simpler to treat than the mixed modes characteristic of anisotropic materials. For wave propagation in directions of symmetry some wave types revert to pure modes, leading to a simpler characteristic equation of lower order. A key condition which we found to facilitate our previous analysis is that at any boundary all wave vectors must lie in the same plane. This requirement implies that the response of the media will be independent of the in-plane coordinate normal to the propagation direction. We therefore conducted all of our analysis in a coordinate system formed by the line load direction and its normals rather than one determined by material symmetry axes. This choice lead to a significant simplification in our algebraic analysis and computations. Compared to the extensive literature on the interaction of plane harmonic waves with anisotropic media, very little work is available on the response of such media to concentrated source loading. Here concentrated sources include point as well as line loads. Harmonically pulsating and transient sources are common types of such loading. Understanding the response of elastic solids to

internal mechanical sources has long been of interest to researchers in classical fields such as acoustics, seismology, as well as modern fields of application like ultrasonics and acoustic emission. It is known that whenever a material undergoes a local failure, elastic waves are generated due to the rapid release of localized strain energy. Such radiation, for example, is known as acoustic emission in the field of nondestructive testing of materials. In seismology it is of course known by the earthquake.

A quick review of available literature on this subject reveals that most of the work done so far is carried out on isotropic media. The effect of imposed line load in homogeneous isotropic media has been discussed by several investigators ever since Lord Rayleigh discovered the existence of surface waves on the surfaces of solids [10]. An account of the literature dealing with this problem through 1957 can be found in Ewing, Jardetsky and Press [18]. Most of the earlier work [13-15] followed Lamb [11,12], who apparently was the first to consider the motion of semi-infinite space caused by a vertically applied line load on the free surface or within the medium. He was able to show that displacements at large distance consists of a series of events which corresponds to the arrival of P-, S-, and Rayleigh surface wave. The analytical approach used in the above mentioned investigations and others [13-15] can be summarized as follows ; the steady state problem for harmonic waves propagating in infinite isotropic media is solved at first and then generalized to the case of half-space using superposition technique. For transient source loading results can be obtained from those corresponding to harmonic ones by a Fourier integral approach.

In this paper, we closely follow the formal developments in our previous works [1-6] and study the response of several anisotropic systems to harmonically pulsating buried line loads. These include infinite, semi-spaces and plate

systems. Our analysis will be carried out on anisotropic media possessing monoclinic or higher symmetry. The load will be in the form of a normal stress load acting at an arbitrary direction within the materials in the plane of symmetry. We use a building block approach in which we start by driving results for an infinite media. Subsequently we obtain the results for half-spaces by using superposition of the infinite medium solution together a scattered solution from the boundary. The sum of both solutions has to satisfy stress free boundary conditions thereby leading to complete solution. Lastly we proceed to develop solutions for a plate by insuring both the infinite media solution and the scattering solution to satisfy the two free surface of the plate. Our work will be easily executed by using the linear transformation approach in which we identify the line load with the x_2 direction. This implies that all involved field variables will be independent of the x_2 direction. Nevertheless, and in general we will have three nonvanishing particle displacements. Material systems of higher symmetry, such as orthotropic, transversely isotropic, cubic, and isotropic are contained implicitly in our analysis. The equivalent crystal systems of monoclinic, orthohombic, hexagonal and cubic may be substituted for the elastic material systems analyzed here. We demonstrate numerical results results drawn from concrete examples of materials belonging to several of these symmetry groups. For orthotropic and higher symmetry materials where the remaining two principal axes lie in the plane of the plate, the particle motions in the saggital and the normal to it uncouple if propagation occurs along either of these in-plane axes.

1.2 Theoretical development

Consider an infinite anisotropic elastic medium possessing monoclinic symmetry. The medium is oriented with respect to the reference cartesian coordinate

system $x_i' = (x_1', x_2', x_3')$ such that the x_3' is assumed normal to its plane of symmetry as shown in figure 1. The plane of symmetry defining the monoclinic symmetry is thus coincident with the $x_1' - x_2'$ plane. With respect to this primed coordinate system, the equations of motion in the medium are given by [1]

$$\frac{\partial \sigma_{ij}'}{\partial x_j'} + f_i' = \rho' \frac{\partial^2 u_i'}{\partial t^2} \tag{1.1}$$

and, from the general constitutive relations for anisotropic media,

$$\sigma_{ij}' = c_{ijkl}' e_{kl}', \qquad i,j,k,l = 1,2,3 \tag{1.2}$$

by the specialized expanded matrix form to monoclinic media

$$\begin{pmatrix} \sigma_{11}' \\ \sigma_{22}' \\ \sigma_{33}' \\ \sigma_{23}' \\ \sigma_{13}' \\ \sigma_{12}' \end{pmatrix} = \begin{pmatrix} c_{11}' & c_{12}' & c_{13}' & 0 & 0 & c_{16}' \\ c_{12}' & c_{22}' & c_{23}' & 0 & 0 & c_{26}' \\ c_{13}' & c_{23}' & c_{33}' & 0 & 0 & c_{36}' \\ 0 & 0 & 0 & c_{44}' & c_{45}' & 0 \\ 0 & 0 & 0 & c_{45}' & c_{55}' & 0 \\ c_{16}' & c_{26}' & c_{36}' & 0 & 0 & c_{66}' \end{pmatrix} \begin{pmatrix} e_{11}' \\ e_{22}' \\ e_{33}' \\ \gamma_{23}' \\ \gamma_{13}' \\ \gamma_{12}' \end{pmatrix} \tag{1.3}$$

where we used the standard contracted subscript notations $1 \rightarrow 11$, $2 \rightarrow 22$, $3 \rightarrow 33$, $4 \rightarrow 23$, $5 \rightarrow 13$, and $6 \rightarrow 12$, to replace $c_{ijkl}(i,j,k,l = 1,2,3)$ with $c_{pq}(p,q = 1,2,...,6)$. Thus, c_{45} stands for c_{2313}, for example. Here σ_{ij}', e_{ij}' and u_i' are the components of stress, strain and displacement, respectively, and ρ' is the material density. In Eq. (3), $\gamma_{ij} = 2e_{ij}$ (with $i \neq j$) defines the engineering shear strain components.

In what follows, we study the response of the infinite medium to a uniform harmonic line load applied along a direction that makes an arbitrary azimuthal angle ϕ with the x_1' axis. That is, the direction $\phi = 0$ coincides with the reference coordinate x_1'. Since, as was pointed out in the introduction, the response of the medium to such a wave is independent of the applied line direction, we conduct our analysis in a transformed coordinate system $x_i =$

(x_1, x_2, x_3) formed by a rotation of the plane $x_1' - x_2'$ through the angle o about the x_3' direction. Thus, the direction x_2 will coincide with the line load direction.

Since c_{ijkl} is a fourth order tensor, then for any orthogonal transformation of the primed to the non-primed coordinates, i.e., it transforms according to

$$c_{ijkl} = \beta_{im}\beta_{jn}\beta_{ko}\beta_{lp}c'_{mnop} \tag{1.4}$$

where β_{ij} is the cosine of the angle between x_i' and x_i , respectively. For a rotation of angle o in the $x_1' - x_2'$ plane, the transformation tensor β_{ij} reduces to

$$\beta_{ij} = \begin{vmatrix} \cos\phi & \sin\phi & 0 \\ -\sin\phi & \cos\phi & 0 \\ 0 & 0 & 1 \end{vmatrix} \tag{1.5}$$

If the transformation (5) is applied to Eq.(3), one gets

$$\begin{pmatrix} \sigma_{11} \\ \sigma_{22} \\ \sigma_{33} \\ \sigma_{23} \\ \sigma_{13} \\ \sigma_{12} \end{pmatrix} = \begin{pmatrix} c_{11} & c_{12} & c_{13} & 0 & 0 & c_{16} \\ c_{12} & c_{22} & c_{23} & 0 & 0 & c_{26} \\ c_{13} & c_{23} & c_{33} & 0 & 0 & c_{36} \\ 0 & 0 & 0 & c_{44} & c_{45} & 0 \\ 0 & 0 & 0 & c_{45} & c_{55} & 0 \\ c_{16} & c_{26} & c_{36} & 0 & 0 & c_{66} \end{pmatrix} \begin{pmatrix} e_{11} \\ e_{22} \\ e_{33} \\ \gamma_{23} \\ \gamma_{13} \\ \gamma_{12} \end{pmatrix} \tag{1.6}$$

where the relations between the c_{pq} and c'_{pq} entries are listed in [5]. Notice that, no matter what rotational angle ϕ is used, the zero entries in Eq.(3) will remain zero in Eq.(6). In terms of the rotated coordinate system x_k, we also write the momentum equations as

$$\frac{\partial \sigma_{ij}}{\partial x_j} + f_i = \rho \frac{\partial^2 u_i}{\partial t^2} \tag{1.7}$$

As mentioned earlier, in the rotated system, the elastic wave equations, for wave propagating in the $x_1 - x_3$ plane, are independent of x_2 . Nevertheless, the particle motion can generally have three nonzero components u_1, u_2, and

u_3. We identify the u_2 displacement as belonging to the horizontally polarized (SH) wave. Here, the equations describing these three wave motions are coupled, complicating the analysis of free waves in the medium. In terms of the displacement components the equations are written in the expanded form

$$\begin{aligned}
[c_{11}\frac{\partial^2}{\partial x_1^2}+c_{55}\frac{\partial^2}{\partial x_3^2}]u_1+[c_{16}\frac{\partial^2}{\partial x_1^2}+c_{45}\frac{\partial^2}{\partial x_3^2}]u_2 & \\
+\frac{\partial}{\partial x_3}[(c_{13}+c_{55})\frac{\partial}{\partial x_1}]u_3 &= \rho\frac{\partial^2 u_1}{\partial t^2}-f_1 \quad (8a)\\
[c_{16}\frac{\partial^2}{\partial x_1^2}+c_{45}\frac{\partial^2}{\partial x_3^2}]u_1+[c_{66}\frac{\partial^2}{\partial x_1^2}+c_{44}\frac{\partial^2}{\partial x_3^2}]u_2 & \\
+\frac{\partial}{\partial x_3}[(c_{36}+c_{45})\frac{\partial}{\partial x_1}]u_3 &= \rho\frac{\partial^2 u_2}{\partial t^2}-f_2 \quad (8b)\\
\frac{\partial}{\partial x_3}[(c_{13}+c_{55})\frac{\partial}{\partial x_1}]u_1+\frac{\partial}{\partial x_3}[(c_{36}+c_{45})\frac{\partial}{\partial x_2}]u_2 & \\
+[c_{55}\frac{\partial^2}{\partial x_1^2}+c_{33}\frac{\partial^2}{\partial x_3^2}]u_3 &= \rho\frac{\partial^2 u_3}{\partial t^2}-f_3 \quad (8c)
\end{aligned}$$

with

$$f_i = Q_i\delta(x_1)\delta(x_3)F(t) \tag{1.9}$$

1.3 Source characterization

Using the above geometric arrangement we proceed to describe the line load by a direc delta body force function located at the arbitrary location ($x_3 = x_3^p$). This choice of source location is arbitrary and is not necessary for the cases of propagation in either the infinite nor the semi-infinite media. However, as will be shown, this choice will lead to great simplification in the algebraic manipulation for the propagation in the plate. Solutions to the present problem can be accomplished by following the procedure used by Achenbach [20]. According to this procedure, the infinite space can be thought of as consisting

of two semi-spaces whose artificial interface contains the applied load. Thus the upper half-space occupies the region $x_3 \geq x_3^p$ whereas the lower half-space occupies the region $x_3 \leq x_3^p$. As a result of this, appropriate condition must be specified at the artificial interface.

In order to be able to specify these interface conditions we consider a very thin "interface" layer extending from $x_3 = x_3^p - o$ to $x_3 = x_3^p + o$. We then start by requiring continuity on the displacement components and their time derivatives, namely

$$u_i(x_1, x_3, t)|_{x_3^p - o}^{x_3^p + o} = 0 \tag{10a}$$

$$\frac{\partial^{(n)} u_i(x_1, x_3, t)}{\partial t^{(n)}}|_{x_3^p - o}^{x_3^p + o} = 0, \quad i = 1, 2, 3 \tag{10b}$$

Integrating Eqs.(8a,b,c) across the interface layer and using the continuity equations(10a,b), leads to the discontinuity in the displacement spatial derivatives resulting in the following jump conditions.

$$(c_{55}\frac{\partial u_1}{\partial x_3} + c_{45}\frac{\partial u_2}{\partial x_3})|_{x_3^p - o}^{x_3^p + o} = -Q_1\delta(x_1)F(t) \tag{11a}$$

$$(c_{45}\frac{\partial u_1}{\partial x_3} + c_{44}\frac{\partial u_2}{\partial x_3})|_{x_3^p - o}^{x_3^p + o} = -Q_2\delta(x_1)F(t) \tag{11b}$$

$$c_{33}\frac{\partial u_3}{\partial x_3}|_{x_3^p - o}^{x_3^p + o} = -Q_3\delta(x_1)F(t) \tag{11c}$$

Now, let's consider the special case where $Q_1 = Q_2 = 0$ and $Q_3 = Q$. For this situation equations (11) reduce to.

$$(c_{55}\frac{\partial u_1}{\partial x_3} + c_{45}\frac{\partial u_2}{\partial x_3})|_{x_3^p - o}^{x_3^p + o} = 0 \tag{12a}$$

$$(c_{45}\frac{\partial u_1}{\partial x_3} + c_{44}\frac{\partial u_2}{\partial x_3})|_{x_3^p - o}^{x_3^p + o} = 0 \tag{12b}$$

$$c_{33}\frac{\partial u_3}{\partial x_3}|_{x_3^p - o}^{x_3^p + o} = \sigma_{33}|_{x_3^p - o}^{x_3^p + o} = -Q\delta(x_1)F(t) \tag{12c}$$

Examination of the relations (12a,b) reveals that, if $(c_{44}c_{55} - c_{45}^2)$ does not vanish (which is the case), then u_1 and u_2 must be at least constant and, in accordance with (10), equal. We choose this constant as zero and thus conclude that u_1 and u_2 vanish at the interface. Finally, we satisfy the normal stress discontinuity condition (13c) by assigning

$$c_{33}\frac{\partial u_3}{\partial x_3}|_{x_3^p+o} = -Q\delta(x_1)F(t)/2, \quad c_{33}\frac{\partial u_3}{\partial x_3}_{x_3^p-o} = Q\delta(x_1)F(t)/2 \quad (1.13)$$

Collecting the above conditions we finally summarize the condition at the artificial interface as

$$\left.\begin{array}{l} u_1 = 0 \\ u_2 = 0 \\ c_{33}\dfrac{\partial u_3}{\partial x_3} = -\dfrac{1}{2}Q\delta(x_1)F(t) \end{array}\right\}, \qquad \text{for } x_3 \geq x_3^p \text{ at } x_3 = x_3^p \qquad (1.14)$$

$$\left.\begin{array}{l} u_1 = 0 \\ u_2 = 0 \\ c_{33}\dfrac{\partial u_3}{\partial x_3} = \dfrac{1}{2}Q\delta(x_1)F(t) \end{array}\right\}, \qquad \text{for } x_3 \leq x_3^p \text{ at } x_3 = x_3^p \qquad (1.15)$$

1.4 Formal solution

Following the procedure of [1], we outline the steps leading to a formal solutions of Eqs.(8a,b,c) for each of the two semi-spaces. Since the body force has been replaced by a "boundary" condition, we drop f_i from Eqs(8a,b,c). We then assume harmonic solutions followed by applying the Fourier transform to these equations in accordance with

$$u_q = \bar{u}_q e^{j\omega t} \qquad (16a)$$

$$\hat{u}_q = \int_{-\infty}^{\infty} \bar{u}_q e^{-j\xi x_1} dx_1 \qquad (16b)$$

The general solution of the resulting differential equations is then sought in the form

$$\hat{u}_i = U_i e^{-\alpha x_3}, \quad i = 1, 2, 3 \tag{1.17}$$

leading to the characteristic equation

$$\begin{pmatrix} \Lambda_{11} & \Lambda_{12} & \Lambda_{13} \\ \Lambda_{12} & \Lambda_{22} & \Lambda_{23} \\ \Lambda_{13} & \Lambda_{23} & \Lambda_{33} \end{pmatrix} \begin{pmatrix} U_1 \\ U_2 \\ U_3 \end{pmatrix} = 0 \tag{1.18}$$

where the various entries Λ_{ij} are given in Appendix A. Note from (18) that the Λ_{ij} matrix is symmetric.

For the existence of nontrivial solutions in U_i the determinant in Eq. (18), must vanish giving an algebraic equation relating α to ω. This is obviously an alternative presentation of Christoffel equation[1]. The difference is that we are now solving for α in terms of ω as compared with solving for the phase velocity for a given propagation direction. Setting the determinant equal to zero, one obtains a sixth order equation in α (cubic in α^2) which is written symbolically as

$$A_1\alpha^6 + A_2\alpha^4 + A_3\alpha^2 + A_4 = 0 \tag{1.19}$$

with its coefficients are given in Appendix B. Eq.(19) admits six solutions for α. These α's have the further properties that

$$\alpha_2 = -\alpha_1, \ \alpha_4 = -\alpha_3, \ \alpha_6 = -\alpha_5 \tag{1.20}$$

Furthermore for each α, equation(18) yields the displacement amplitude ratios $v_q = U_{2q}/U_{1q}, w_q = U_{3q}/U_{1q}$

$$v_q = -\frac{\Lambda_{11}\Lambda_{23} - \Lambda_{12}\Lambda_{13}}{\Lambda_{12}\Lambda_{23} - \Lambda_{22}\Lambda_{13}} \tag{21a}$$

$$w_q = -\frac{\Lambda_{12}\Lambda_{23} - \Lambda_{13}\Lambda_{22}}{\Lambda_{23}\Lambda_{23} - \Lambda_{22}\Lambda_{33}} \tag{21b}$$

Finally, using superposition, we write the formal solutions for the displacements of equations (8a,b,c) and their associated stress components using Eq.(6) as

$$(\hat{u}_1, \hat{u}_2, \hat{u}_3) = \sum_{q=1}^{6} (1, v_q, w_q) U_{1q} e^{-\alpha_q (x_3 - x_3^p)} \tag{1.22}$$

$$(\hat{\sigma}_{33}, \hat{\sigma}_{13}, \hat{\sigma}_{23}) = \sum_{q=1}^{6} (D_{1q}, D_{2q}, D_{3q}) U_{1q} e^{-\alpha_q (x_3 - x_3^p)} \tag{1.23}$$

where

$$D_{1q} = j\xi(c_{13} + c_{36} v_q) - c_{33} \alpha_q w_q \tag{1.24}$$

$$D_{2q} = c_{55}(j\xi w_q - \alpha_q) - c_{45} \alpha_q v_q \tag{1.25}$$

$$D_{3q} = c_{45}(j\xi w_q - \alpha_q) - c_{44} \alpha_q v_q, \qquad q = 1, 2, .., 6 \tag{1.26}$$

With reference to equation the relation (20) and to the Λ_{ij} entries of Appendix A and by inspection of equations (20) and (24-26), one recognizes the relations (see Ref.[2])

$$\begin{array}{llllll} v_2 & = v_1, & v_4 & = -v_3, & v_6 & = v_5 \\ w_2 & = -w_1, & w_4 & = -w_3, & w_6 & = -w_5 \\ D_{12} & = D_{11}, & D_{14} & = D_{13}, & D_{16} & = D_{15} \\ D_{22} & = -D_{21}, & D_{24} & = -D_{23}, & D_{26} & = -D_{25} \\ D_{32} & = -D_{31}, & D_{34} & = -D_{33}, & D_{36} & = -D_{35} \end{array} \tag{1.27}$$

The above solutions with their various properties can now be specialized to both artificial half-spaces by the following steps. Inspection of the above solutions indicate that each consists of three pairs of wave components, each pair propagating in mirror image fashion with respect to the interface, namely along positive and negative x_3-directions. Since propagation is expected to emanate from the interface into both media, we arbitrary reserve q_1, q_3, and

q_5 for the lower half-space; the remaining one's, namely described with q_2, q_4, and q_6 for the upper one. We list the formal solution in the lower and lower half-spaces according to

$$\left.\begin{aligned}(\hat{u}_1, \hat{u}_2, \hat{u}_3) &= \sum_{q=1,3,5} (1, v_q, w_q) U_{1q} e^{-\alpha_q (x_3 - x_3^P)} \\ (\hat{\sigma}_{33}, \hat{\sigma}_{13}, \hat{\sigma}_{23}) &= \sum_{q=1,3,5} (D_{1q}, D_{2q}, D_{3q}) U_{1q} e^{-\alpha_q (x_3 - x_3^P)}\end{aligned}\right\} \quad x_3 \geq x_3^P \qquad (1.28)$$

$$\left.\begin{aligned}(\hat{u}_1, \hat{u}_2, \hat{u}_3) &= \sum_{q=2,4,6} (1, v_q, w_q) U_{1q} e^{-\alpha_q (x_3 - x_3^P)} \\ (\hat{\sigma}_{33}, \hat{\sigma}_{13}, \hat{\sigma}_{23}) &= \sum_{q=2,4,6} (D_{1q}, D_{2q}, D_{3q}) U_{1q} e^{-\alpha_q (x_3 - x_3^P)}\end{aligned}\right\} \quad x_3 \leq x_3^P \qquad (1.29)$$

1.5 Solutions in infinite media

At this point, we have presented a formal solution of the field equation in a monoclinic medium. The amplitudes U_{1q} are the unknowns. The amplitudes U_{1q} will now be determined by implementing the artificial interface conditions (14-15). To this end, if (28) is subjected to the conditions (14) and (29) to (15), one finally solves the displacement amplitudes as

$$U_{11} = -U_{12} = (v_5 - v_3) Q / (2 c_{33} D_{um}) \qquad (30a)$$

$$U_{13} = -U_{14} = (v_1 - v_5) Q / (2 c_{33} D_{um}) \qquad (30b)$$

$$U_{15} = -U_{16} = (v_3 - v_1) Q / (2 c_{33} D_{um}) \qquad (30c)$$

where

$$D_{um} = v_1(\alpha_3 w_3 - \alpha_5 w_5) + v_3(\alpha_5 w_5 - \alpha_1 w_1) + v_5(\alpha_1 w_1 - \alpha_3 w_3) \qquad (1.31)$$

It is interesting to note that $D_{um} = 0$ defines an equivalent Christoffel characteristic equation for the propagation of bulk waves in the medium [-]. With

these solutions for the wave amplitudes, solutions in the upper region can be written in terms of $q = 1, 3, 5$ as

$$\begin{aligned}(\hat{u}_1, \hat{u}_2, \hat{u}_3) &= \sum_{q=1,3,5} (-1, -v_q, w_q) U_{1q} e^{-\alpha_q (x_3^p - x_3)} \\ (\hat{\sigma}_{33}, \hat{\sigma}_{13}, \hat{\sigma}_{23}) &= \sum_{q=1,3,5} (-D_{1q}, D_{2q}, D_{3q}) U_{1q} e^{-\alpha_q (x_3^p - x_3)}\end{aligned} \tag{1.32}$$

In summary, solutions (28) and (32) with the amplitude solutions (30) uniquely define the propagation fields in the lower and upper "artificial" semi-spaces. In other words, their combination constitute the total solutions for the infinite medium.

1.6 Solution in half-spaces

We now adapt the solutions of the infinite media (28) and (32) to solve for the case where the free boundary is intercepts the propagating pulse at some arbitrary location parallel to the plane $x_3 = 0$. We assume that the free boundary is located at $x_3 = -d$ as depicted in figure 2. This implies that the free boundary is located in the upper region and thus can only interfere with the propagation fields in the negative x_3 direction. For this case, the solution (32) will constitute an incident wave on free surface. As a results waves will reflect from the free boundary and propagate in the positive x_3 direction. Thus, appropriate formal solutions for the reflected waves can be adapted from the solution (28) in accordance with (Note now that x_3^p does not appear because solutions are referred to the origin $x_3 = 0$)

$$(\hat{u}_1^r, \hat{u}_2^r, \hat{u}_3^r) = \sum_{q=1,3,5} (1, v_q, w_q) U_{1q}^r e^{-\alpha_q x_3} \tag{1.33}$$

$$(\hat{\sigma}_{33}^r, \hat{\sigma}_{13}^r, \hat{\sigma}_{23}^r) = \sum_{q=1,3,5} (D_{1q}, D_{2q}, D_{3q}) U_{1q}^r e^{-\alpha_q x_3} \tag{1.34}$$

With this the total solution for the semi-space (designated with superscript 's') which is required to satisfy the stress free boundary condition is obtained by superposing the incident waves and reflected waves in accordance with

$$\begin{aligned}(\hat{u}_1^s, \hat{u}_2^s, \hat{u}_3^s) &= \sum_{q=1,3,5} (-1, -v_q, w_q) U_{1q}^{r(i)} e^{-\alpha_q (x_3^p - x_3)} \\ &+ \sum_{q=1,3,5} (1, v_q, w_q) U_{1q}^r e^{-\alpha_q x_3}\end{aligned} \tag{1.35}$$

$$\begin{aligned}(\hat{\sigma}_{33}^s, \hat{\sigma}_{13}^s, \hat{\sigma}_{23}^s) &= \sum_{q=1,3,5} (-D_{1q}, D_{2q}, D_{3q}) U_{1q}^{(i)} e^{-\alpha_q (x_3^p - x_3)} \\ &+ \sum_{q=1,3,5} (D_{1q}, D_{2q}, D_{3q}) U_{1q}^r e^{-\alpha_q x_3}\end{aligned} \tag{1.36}$$

The boundary condition is given by

$$\hat{\sigma}_{13}^s = \hat{\sigma}_{23}^s = \hat{\sigma}_{33}^s = 0, \quad \text{at } x_3 = -d \tag{1.37}$$

By imposing the boundary conditions (37) on Eq.(6), linear system is obtained by

$$\begin{pmatrix} D_{11} & D_{13} & D_{15} \\ D_{21} & D_{23} & D_{25} \\ D_{31} & D_{33} & D_{35} \end{pmatrix} \begin{pmatrix} U_{11}^r E_1 \\ U_{13}^r E_3 \\ U_{15}^r E_5 \end{pmatrix} = \begin{pmatrix} R_1 \\ R_3 \\ R_5 \end{pmatrix} \tag{1.38}$$

where

$$R_1 = -(U_{11}^{(i)} D_{11} E_1^r + U_{13}^{(i)} D_{13} E_3^r + U_{15}^{(i)} D_{15} E_5^r) \tag{39a}$$

$$R_3 = (U_{11}^{(i)} D_{21} E_1^r + U_{13}^{(i)} D_{23} E_3^r + U_{15}^{(i)} D_{25} E_5^r) \tag{39b}$$

$$R_5 = (U_{11}^{(i)} D_{31} E_1^r + U_{13}^{(i)} D_{33} E_3^r + U_{15}^{(i)} D_{35} E_5^r) \tag{39c}$$

Using the standard Cramer's rule we solve the reflected amplitudes as

$$U_{11}^r = \frac{1}{D_{sm} E_1} (R_1 G_{11} - R_3 G_{21} + R_5 G_{31}) \tag{40a}$$

$$U_{13}^r = \frac{-1}{D_{sm} E_3} (R_1 G_{13} - R_3 G_{23} + R_5 G_{33}) \tag{40b}$$

$$U_{15}^r = \frac{1}{D_{sm}E_5}(R_1G_{15} - R_3G_{25} + R_5G_{35}) \tag{40c}$$

with

$$E_q = e^{\alpha_q d}, E_q^r = e^{-\alpha_q(x_3^p+d)}, \qquad \text{q=1,3,5} \tag{1.41}$$

and

$$D_{sm} = D_{11}G_{11} - D_{21}G_{21} + D_{31}G_{31} \tag{1.42}$$

where G_{qr} are given in Appendix B. It is worth noting that $D_{sm} = 0$ defines the characteristic equations for the propagation of Rayleigh (surface) wave on the free surface [1]

1.7 Solution for infinite plates

We now consider the response to the line load in an infinite plates having the thickness 2d. Since the elastic waves in the plates are reflected at both free boundaries $x_3 = d$ and $x_3 = -d$ as shown in figure 3, the solutions are obviously more complicated than for the half space case, we however, the solution procedures are the same. To this end, we adapt the solutions of the infinite space (28,32) in order to solve for the case where the both free boundaries intercept the propagating field. This implies that the free boundaries are in the upper and lower semi-space and interfere with the propagation in the negative and positive x_3 directions. For this case, the both upgoing and downgoing waves in the infinite space will constitute incident waves. As a result upgoing waves will reflect from the free boundary $x_3 = -d$ and propagate in the positive x_3 direction whereas downgoing waves will reflect from the free boundary $x_3 = d$ and propagate in the negative x_3 direction. Thus, total formal solutions for the plate (designated with superscript 'p') can be adapted from the

solution for the infinite space and free waves (i.e. the six scattered ones) in accordance with

for the upper artificial layer $(-d \le x_3 \le x_3^p)$

$$\begin{aligned}(\hat{u}_1^p, \hat{u}_2^p, \hat{u}_3^p) &= \sum_{q=1,3,5} (-1, -v_q, w_q) U_{1q}^{(i)} e^{-\alpha_q (x_3^p - x_3)} \\ &\quad + \sum_{q=1}^{6} (1, v_q, w_q) U_{1q}^{r} e^{-\alpha_q x_3}\end{aligned} \tag{1.43}$$

$$\begin{aligned}(\hat{\sigma}_{33}^p, \hat{\sigma}_{13}^p, \hat{\sigma}_{23}^p) &= \sum_{q=1,3,5} (-D_{1q}, D_{2q}, D_{3q}) U_{1q}^{(i)} e^{-\alpha_q (x_3^p - x_3)} \\ &\quad + \sum_{q=1}^{6} (D_{1q}, D_{2q}, D_{3q}) U_{1q}^{r} e^{-\alpha_q x_3}\end{aligned} \tag{1.44}$$

for the lower artificial layer $(x_3^p \le x_3 \le d)$

$$\begin{aligned}(\hat{u}_1^p, \hat{u}_2^p, \hat{u}_3^p) &= \sum_{q=1,3,5} (1, v_q, w_q) U_{1q}^{(i)} e^{-\alpha_q (x_3 - x_3^p)} \\ &\quad + \sum_{q=1}^{6} (1, v_q, w_q) U_{1q}^{r} e^{-\alpha_q x_3}\end{aligned} \tag{1.45}$$

$$\begin{aligned}(\hat{\sigma}_{33}^p, \hat{\sigma}_{13}^p, \hat{\sigma}_{23}^p) &= \sum_{q=1,3,5} (D_{1q}, D_{2q}, D_{3q}) U_{1q}^{(i)} e^{-\alpha_q (x_3 - x_3^p)} \\ &\quad + \sum_{q=1}^{6} (D_{1q}, D_{2q}, D_{3q}) U_{1q}^{r} e^{-\alpha_q x_3}\end{aligned} \tag{1.46}$$

The polarized amplitude, U_{1q}^r, is again determined by applying the free traction on the free surfaces given by

$$\hat{\sigma}_{33}^p = \hat{\sigma}_{13}^p = \hat{\sigma}_{23}^p = 0, \qquad \text{at } x_3 = \pm d \tag{1.47}$$

Now, substituting the solution for the plate (??,??) into (??) with the aid of (27) yields a linear system to be

$$\begin{pmatrix} D_{11}E_1 & D_{13}E_3 & D_{15}E_5 & D_{11}\bar{E}_1 & D_{13}\bar{E}_3 & D_{15}\bar{E}_5 \\ D_{21}E_1 & D_{23}E_3 & D_{25}E_5 & -D_{21}\bar{E}_1 & -D_{23}\bar{E}_3 & -D_{25}\bar{E}_5 \\ D_{31}E_1 & D_{33}E_3 & D_{35}E_5 & -D_{31}\bar{E}_1 & -D_{33}\bar{E}_3 & -D_{35}\bar{E}_5 \\ D_{11}\bar{E}_1 & D_{13}\bar{E}_3 & D_{15}\bar{E}_5 & D_{11}E_1 & D_{13}E_3 & D_{15}E_5 \\ -D_{21}\bar{E}_1 & -D_{23}\bar{E}_3 & -D_{25}\bar{E}_5 & D_{21}E_1 & D_{23}E_3 & D_{25}E_5 \\ -D_{31}\bar{E}_1 & -D_{33}\bar{E}_3 & -D_{35}\bar{E}_5 & D_{31}E_1 & D_{33}E_3 & D_{35}E_5 \end{pmatrix} \begin{pmatrix} U_{11}^r \\ U_{13}^r \\ U_{15}^r \\ U_{12}^r \\ U_{14}^r \\ U_{16}^r \end{pmatrix} = \begin{pmatrix} R_1 \\ R_3 \\ R_5 \\ R_2 \\ R_4 \\ R_6 \end{pmatrix} \tag{1.48}$$

where, besides the definitions of R_1, R_3, and R_5 of (39),

$$R_2 = (U_{11}^{(i)} D_{11} \bar{E}_1^r + U_{13}^{(i)} D_{13} \bar{E}_3^r + U_{15}^{(i)} D_{15} \bar{E}_5^r) \quad (49a)$$

$$R_4 = (U_{11}^{(i)} D_{21} \bar{E}_1^r + U_{13}^{(i)} D_{23} \bar{E}_3^r + U_{15}^{(i)} D_{25} \bar{E}_5^r) \quad (49b)$$

$$R_6 = (U_{11}^{(i)} D_{31} \bar{E}_1^r + U_{13}^{(i)} D_{33} \bar{E}_3^r + U_{15}^{(i)} D_{35} \bar{E}_5^r) \quad (49c)$$

with

$$\bar{E}_q = e^{-\alpha_q d}, \quad \bar{E}_q^r = e^{-\alpha_q (d - x_3^p)}, \qquad \text{q=1,3,5} \quad (1.50)$$

After straight forward algebraic manipulation, the amplitude U_{1q}^r is algebraically simplified to

$$U_{11}^r = -U_{12}^r = Q \frac{\sinh(\alpha_3 d)\sinh(\alpha_5 d)}{D_{pm} \coth(\alpha_5 d) D_{15}^2} [(R_{11}H_{11} - R_{22}H_{12})(H_{52}H_{41} - H_{51}H_{42}) - (R_{33}H_{41} - R_{44}H_{42})(H_{22}H_{11} - H_{12}H_{21})] \quad (51a)$$

$$U_{13}^r = -U_{14}^r = -Q \frac{\sinh(\alpha_1 d)\sinh(\alpha_5 d)}{D_{pm} \coth(\alpha_5 d) D_{15}^2} [(R_{11}H_{21} - R_{22}H_{22})(H_{42}H_{51} - H_{41}H_{52}) - (R_{33}H_{51} - R_{44}H_{52})(H_{12}H_{21} - H_{11}H_{22})] \quad (51b)$$

$$U_{15}^r = -U_{16}^r = Q \frac{\sinh(\alpha_1 d)\sinh(\alpha_3 d)}{D_{pm} \coth(\alpha_3 d) D_{13}^2} [(R_{11}H_{31} - R_{22}H_{31})(H_{42}H_{61} - H_{41}H_{62}) - (R_{33}H_{61} - R_{44}H_{62})(H_{12}H_{31} - H_{11}H_{32})] \quad (51c)$$

with

$$D_{pm} = -4\cosh(\alpha_1 d)\cosh(\alpha_3 d)\cosh(\alpha_5 d) \times [D_{11}G_{11}\coth(\alpha_1 d) - D_{13}G_{13}\coth(\alpha_3 d) + D_{15}G_{15}\coth(\alpha_5 d)] \times [D_{11}G_{11}\tanh(\alpha_1 d) - D_{13}G_{13}\tanh(\alpha_3 d) + D_{15}G_{15}\tanh(\alpha_5 d)] \quad (1.52)$$

where R_{kk} and H_{kl} are given in Appendix B. Note that $D_{pm} = 0$ defines the characteristic equations for the propagation of free wave in the plate.

1.8 Numerical results and discussions

In this section we present numerical illustrations of the above analysis. We choose for our illustration a graphite-epoxy composite material. The microstructure of this particular material has been extensively studied and models predicting its effective anisotropic properties are available elsewhere [1]. Based upon a 60% graphite fiber volume fraction these effective properties are given with respect to the reference coordinate system x_i' as

$$c'_{ij} = \begin{pmatrix} 155.60 & 3.70 & 3.70 & 0 & 0 & 0 \\ 3.70 & 15.95 & 4.33 & 0 & 0 & 0 \\ 3.70 & 4.33 & 15.95 & 0 & 0 & 0 \\ 0 & 0 & 0 & 5.81 & 0 & 0 \\ 0 & 0 & 0 & 0 & 7.46 & 0 \\ 0 & 0 & 0 & 0 & 0 & 7.46 \end{pmatrix} \times 10^{10} \quad [\ \mathrm{N/m^2}\ ]$$

with $\rho = 1.6$ g/cm^3. For a rotation of $\phi = 45°$, for example, these properties transform to

$$c_{ij} = \begin{pmatrix} 51.20 & 36.28 & 4.03 & 0 & 0 & 36.13 \\ 36.28 & 51.20 & 4.03 & 0 & 0 & 36.13 \\ 4.03 & 4.03 & 16.00 & 0 & 0 & 0.31 \\ 0 & 0 & 0 & 6.64 & 0 & 0 \\ 0 & 0 & 0 & 0 & 6.64 & 0 \\ 36.13 & 36.13 & 0.31 & 0 & 0 & 40.02 \end{pmatrix} \times 10^{10} \quad [\ \mathrm{N/m^2}\ ]$$

which confirms the earlier conclusion that the transformed matrix takes the format of monoclinic symmetry. Having chosen the material we now summarize a "flow chart" like procedure for our subsequent calculations. After specifying the azimuthal angle ϕ (namely, the line load direction) we proceed in the first step to evaluate α's for given values of the wavenumber ξ. We then sort out the various α's in accordance with the required format of equation (28-29). In the second step we evaluate the displacement ratios. By now, we

are ready to calculate the inverse transforms in accordance with

$$\bar{u}_i = \frac{1}{2\pi}\int_{-\infty}^{\infty} \hat{u}_i e^{j\xi x_1} d\xi, \qquad i = 1,2,3 \tag{1.53}$$

Depending upon whether $\hat{u}_i$ is symmetric or antisymmetric, computational effort would be greatly reduced. We first would like to present solutions to symmetry situations. If α_q is symmetric with respect to ξ. Then v_q will be symmetric while w_q, D_{iq}, D_{sm}, and D_{pm} will be antisymmetric with respect to ξ. It then follows that $\hat{u}_1$ and $\hat{u}_2$ are symmetric while $\hat{u}_3$ is antisymmetric. Accordingly equation (??) simplifies to

$$\bar{u}_i = \frac{1}{\pi}\int_0^{\infty} j\hat{u}_i \sin(\xi x_1) d\xi, \qquad i = 1,2 \tag{54a}$$

$$\bar{u}_3 = \frac{1}{\pi}\int_0^{\infty} \hat{u}_3 \cos(\xi x_1) d\xi \tag{54b}$$

The calculations of displacement and stress components are then formed straightforward, except at singularities. These singularities are poles corresponding to the zeros of D_{sm} and D_{pm}, namely, the characteristic equations for a surface wave in the halfspace and free waves in the plate, respectively. We find that the poles do not exist in the second and the fourth quadrant of figure 4, namely for $Re(\xi) > 0$ and $Im(\xi) < 0$ and that D_{um} of the infinite medium has no poles. Thus, $\bar{u}_i$ in the infinite space is integrated along the real ξ-axis. Two different procedures have been used in dealing with these poles in the integration process. The first requires the removal of these singularities from the integrals. The second, based upon the work of Neerhoff et al [18]. merely deforms the contour of integration below the real ξ-axis, as shown in figure 4, so that no poles occur on the path of integration. In order to optimize accuracy, judicious choices of the parameter, ξ_i, are required. The value of

ξ_i, imaginary part of ξ_i, needs to be large enough to offset the contributions of singular points, but not two large since it reduces the accuracy. In our calculations, we choose the value $\xi_i = 0.1$. For our numerical illustrations we arbitrary choose the azimuthal angle $\phi = 45°$ and the angular frequency, $\omega = 3.0 \times 10^6$ rad/sec.

Figures 5-7 depict the displacement and a normal stress components $\bar{u}_1, \bar{u}_2, \bar{u}_3, \bar{\sigma}_{33}$ in the media at the location $x_3 = -3$ mm. The location of the line load is chosen at the origin of the x_i coordinate system for all three geometries (infinite- and half-space, plate): thus $\bar{u}_1$ and $\bar{\sigma}_{33}$ are symmetric with respect to x_3 axis while $\bar{u}_1$ and $\bar{u}_2$ are antisymmetric. Note from the figures that the amplitudes of the displacement and stress component are slowly decreasing with oscillations for a long distances from the location of line load in the infinite and semi-infinite space. However, the amplitudes in the plate are oscillating along the location $x_3 = -3$ mm with persisting amplitudes.

Figures 8-10 present the displacement mode $(\bar{u}_1, \bar{u}_3)$ at various locations. We calculate deformation fields at the locations designated by broken various radii (2.4mm, 5.55mm, and 7.2mm in infinite media; 2.4mm and 5.55mm in infinite media; and 4.0mm in the plate) away from the source location. For these investigations the line load is located at the origin of x_i coordinate system in the infinite and half-space media, and at (0,0,1) in the plate. Solid curves represent deformations defined by $x_1 + \bar{u}_1 \times 10^2, x_3 + \bar{u}_3 \times 10^2$. Note that in the infinite media, $\bar{u}_1$ is zero on the x_1 axis and that $\bar{u}_3$ has maximum amplitude on the x_3. However, in the semi-infinite space and the plate the displacement fields are much affected by the reflected waves. The displacement amplitude in the semi-infinite space is seen to be greater than that in the infinite space.

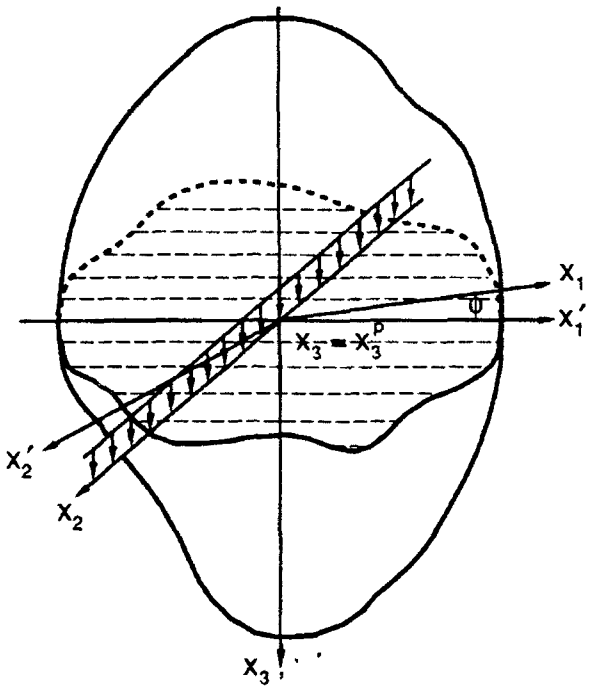

Figure 1.1: A applied line load in an anisotropic infinite media

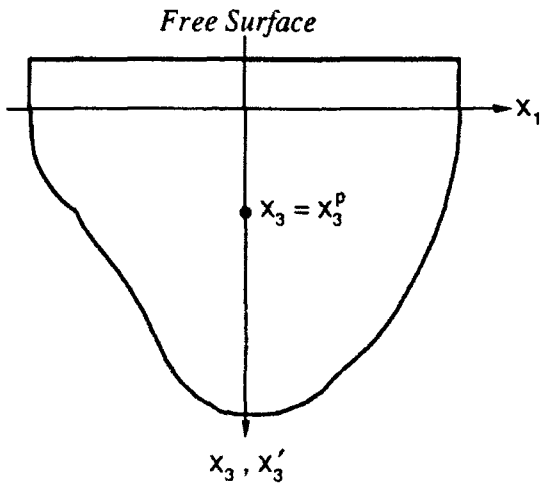

Figure 1.2: Semi-infinite media

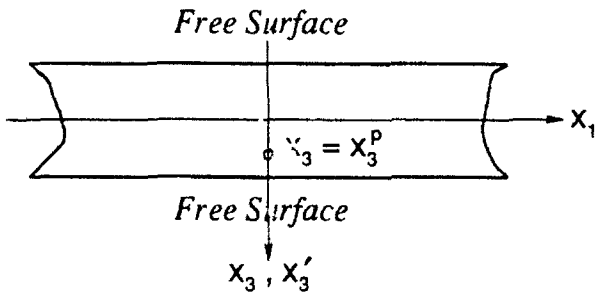

Figure 1.3: The infinite plate

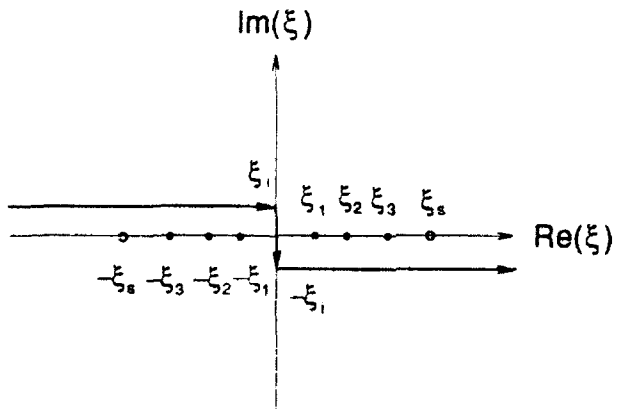

Figure 1.4: Complex integral contour

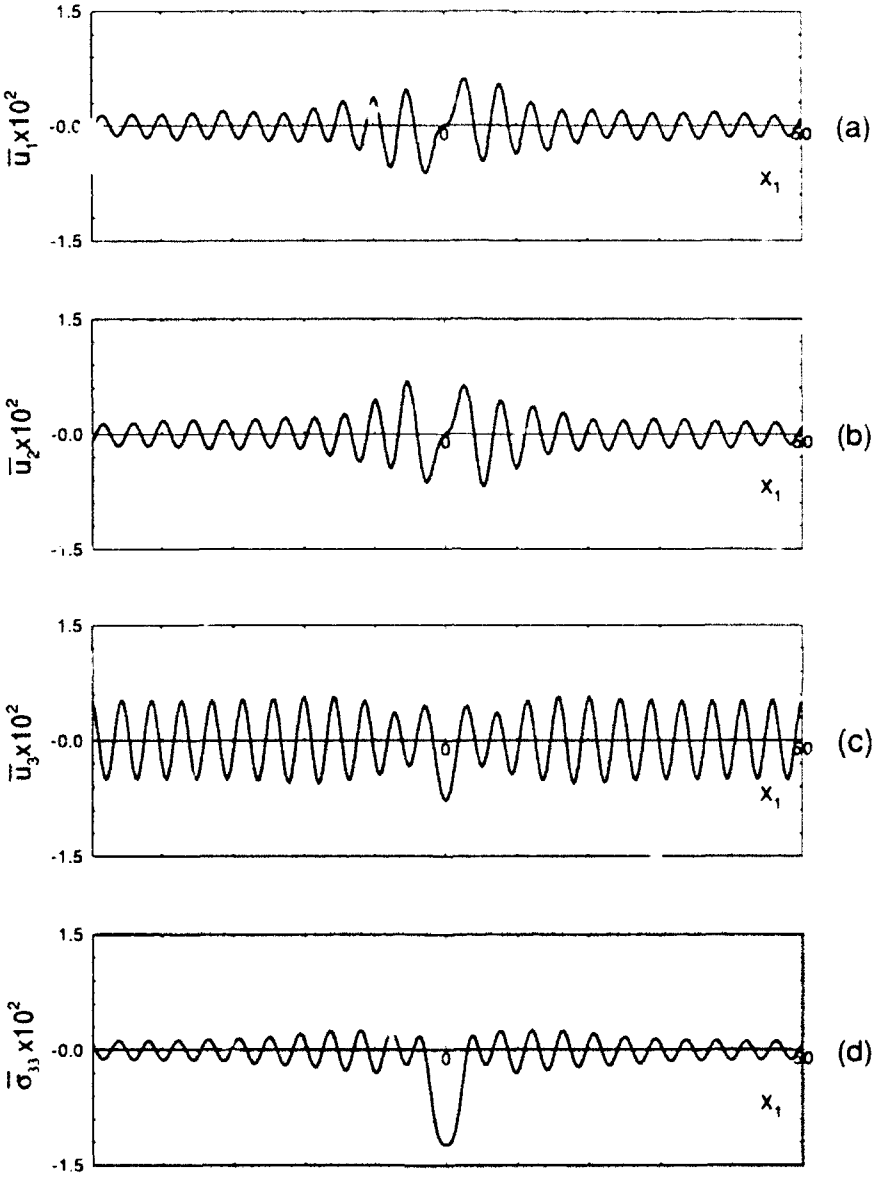

Figure 1.5: Displacements and stress in infinite space of graphite-epoxy at $x_3 = -3$ mm : (a) $\bar{u}_1$, (b) $\bar{u}_2$, (c) $\bar{u}_3$, (d) $\bar{\sigma}_{33}$

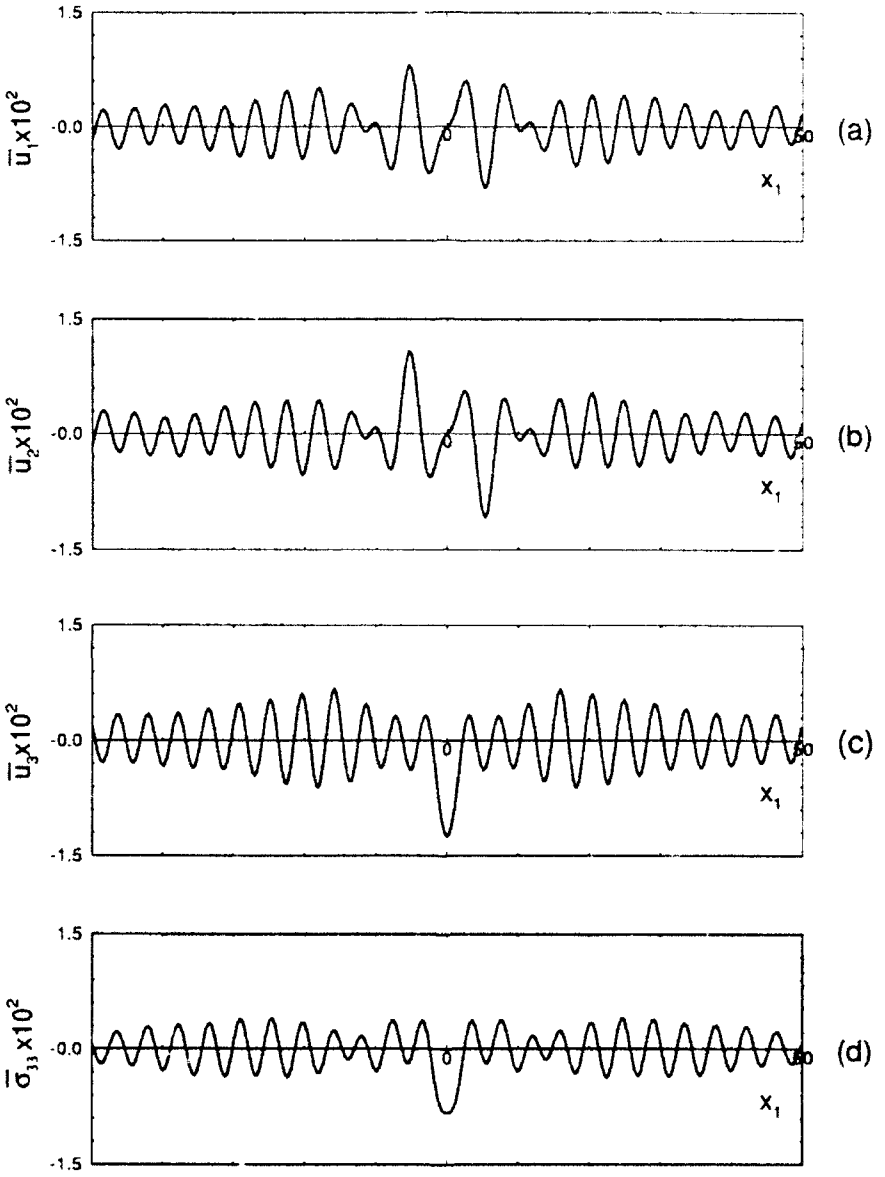

Figure 1.6: Displacements and stress in semi-infinite space of graphite-epoxy at $x_3 = -3$ mm : (a) $\bar{u}_1$, (b) $\bar{u}_2$, (c) $\bar{u}_3$, (d) $\bar{\sigma}_{33}$

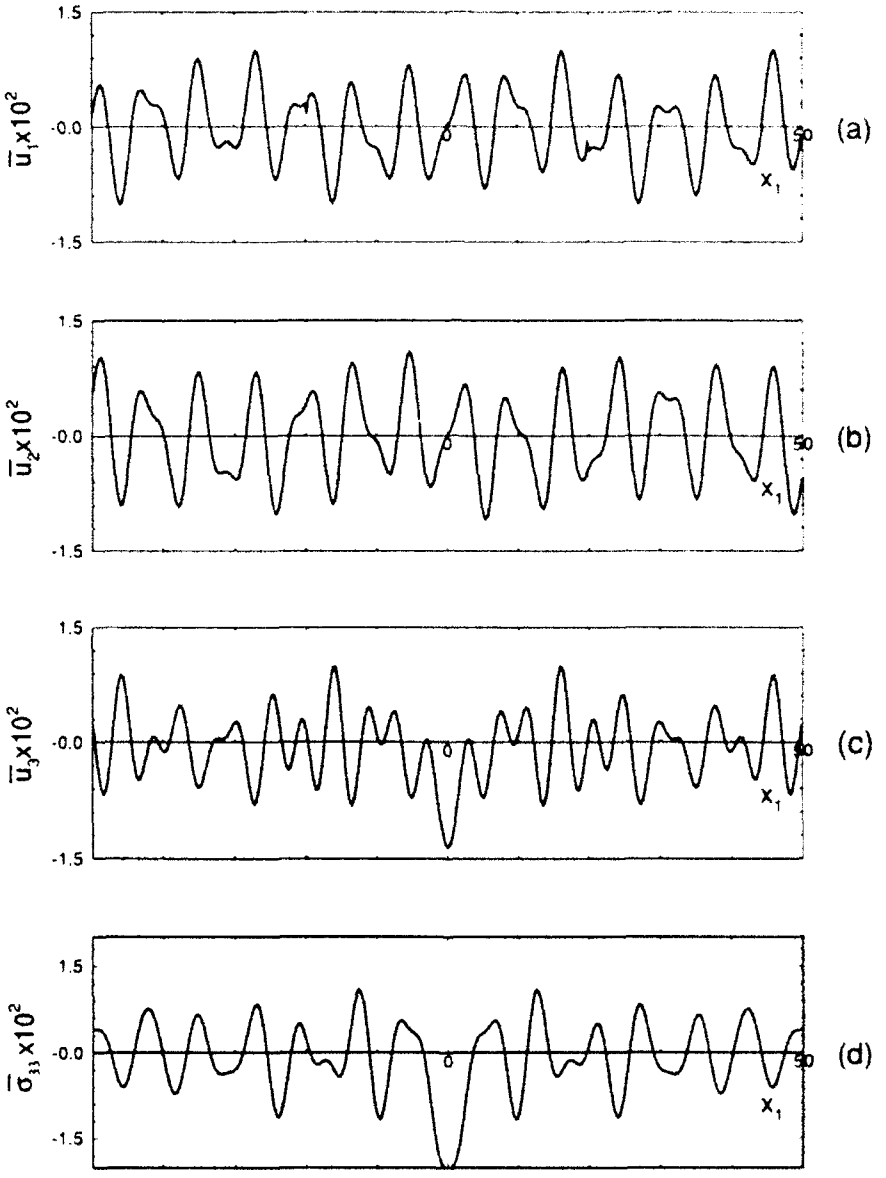

Figure 1.7: Displacements and stress in plate of graphite-epoxy at $x_3 = -3$ mm : (a) $\bar{u}_1$, (b) $\bar{u}_2$, (c) $\bar{u}_3$, (d) $\bar{\sigma}_{33}$

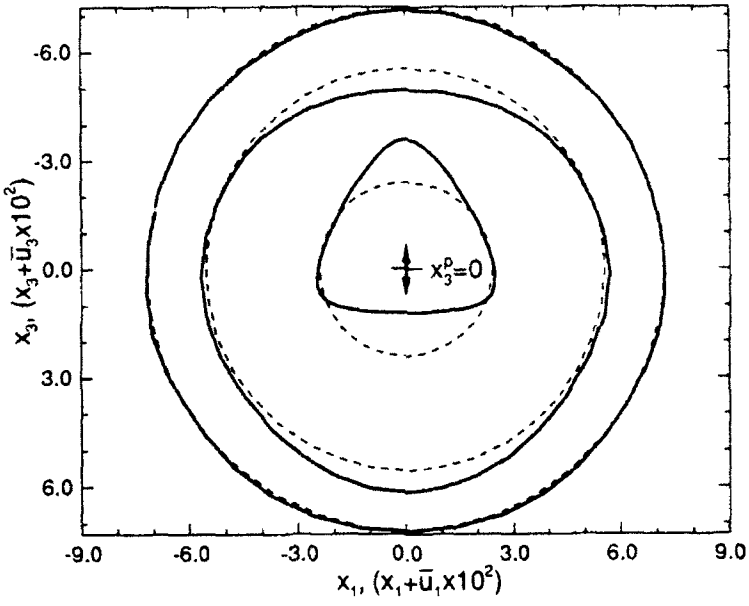

Figure 1.8: Displacement modes in the infinite space of graphite-epoxy. Broken circles are chosen as receiver location (x_1, x_3) and solid curves are displacements modes $(x_1 + \bar{u}_1 \times 10^2, x_3 + \bar{u}_3 \times 10^2)$ with respect to broken circles. The line load is located at (0, 0, 1)

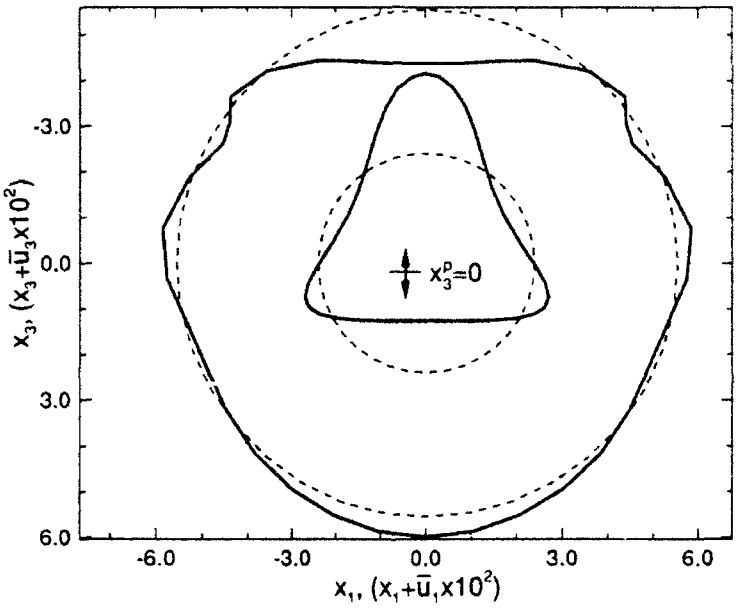

Figure 1.9: Displacement modes in the half-space of graphite-epoxy. Broken circles are chosen as receiver location (x_1, x_3) and solid curves are displacements modes $(x_1 + \bar{u}_1 \times 10^2, x_3 + \bar{u}_3 \times 10^2)$ with respect to broken circles. Free surface is $x_3 = -5.55$ mm and the line load is located at the origin of the system.

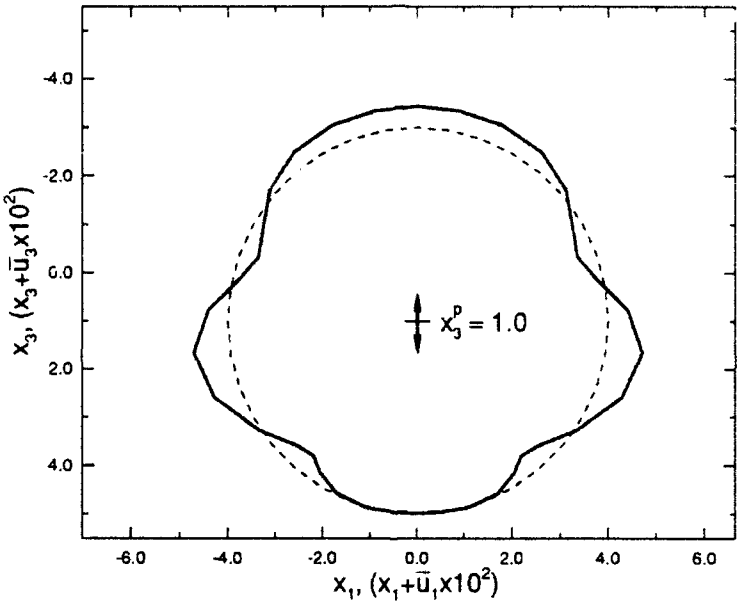

Figure 1.10: Displacement modes in the plate of graphite-epoxy. Broken circle is chosen as receiver location (x_1, x_3) and solid curve is displacement mode $(x_1 + \bar{u}_1 \times 10^2, x_3 + \bar{u}_3 \times 10^2)$ with respect to broken circle. Free surface is $x_3 = \pm 5.55$ mm and the line load is located at (0, 0, 1).

Bibliography

[1] A. H. Nayfeh, "Elastic wave reflection from liquid-anisotropic substrata interfaces," Wave motion, 14, 55-67(1991).

[2] D. E. Chimenti and A. H. Nayfeh, "Ultrasonic Reflection and Guided Waves in Fluid-Coupled Composite Laminates", J. Nondestructive Evaluation, Vol. 9, No. 2/3, (1990)

[3] A. H. Nayfeh and D. E. Chimenti, "Free Wave Propagation in Plates of General Anisotropic Media," J. Appl. Mech., Vol.55, 863-870(1989).

[4] A. H. Nayfeh and D. E. Chimenti, "Ultrasonic Wave Reflection from Liquid-Coupled Orthotropic Plates with Application to Fibrous Composites," J. Appl. Mech., Vol.55, 863-870(1988).

[5] A. H. Nayfeh and D. E. Chimenti, "Propagation of Guided Waves in Fluid-Coupled Plates of Fiber-Reinforced Composites," J. Appl. Mech., Vol.83, pp1736(1988).

[6] D. E. Chimenti and A. H. Nayfeh, "Ultrasonic leaky waves in a solid plate separating fluid and vacuum media," J. Acous. Soc. Am, Vol.

[7] J. L. Synge, "Elastic waves in anisotropic Media", J. Math. Phys., Vol.35, 323-334(1957)

[8] F. I. Fedorov, "Theory of Elastic Waves in Crystals, Plenum, New York, (1968).

[9] M. I. P. Musgrave, "Crystal Acoustics", Holden Day, San Francisco, (1970).

[10] Lord Rayleigh, "On the free vibrations of an infinite plate of homogeneous isotropic elastic materual, Proc. London Mathematical Society, 20, 225 (1889)

[11] H.Lamb, "On the Propagation of Tremors Over the Surface of an Elastic solid", Phil. Trans. Roy. Soc.,London, ser.A, Vol.203, 1-42(1904).

[12] H.Lamb, "On Waves in an Elastic Plate", Phil. Trans. Roy. Soc., London, Ser.A, Vol.93, 114-128(1917)

[13] E. R. Lapwood, "The Disturbance due to a Line Source in a Semi-infinite Elastic Medium", Phil. Trans. Roy. Soc., London, Ser.A, Vol.242, 9-100(1949).

[14] G. Eason, J.Fulton and I. N. Sneddon, "The Generation of Wave in an Infinite Elastic Solid by Variable Body Forces",Phil. Trans. Roy. Soc.,London, Ser.A, Vol.248, 575-308(1956).

[15] C. Pekeris and H. Lifson, "Motion of the Surface of a Uniform Elastic Half-Space Produced by a Buried Pulse", J. Acous. Soc. Am., Vol.29, 1233-1238(1957).

[16] M. Shmuely, "Response of Plates to Transient Source", J. of Sound and Vibration, Vol.32(4), 507-512(1974)

[17] M. Shmuely, "Stress Wave Propagation in Plates Subjected to a Transient Line Source", Int. J. Solid Structure, Vol.11, 679-691(1975)

[18] F. L. Neerhoff, "Diffraction of Love Waves by a Stress Free Crack of Finite With in the Plane Interface of a Layered Composite," Appl. Sci. Res., Vol.35, 265-315(1979).

[19] W. Ewing, W.Jardetzky and F. Press, Elastic Waves in Layered Media. (McGrraw Hill, New york, 1957)

[20] J. P. Achenbach, Wave Propagations in Elastic Solids, (American Elservier Pub. Co., New York, 1973)

[21] Y. C. Fung, Foundation of Solid Mechanics. (Prentice-Hall, Englewood Cliffs, N. J. 1965)

Appendix A

Various coefficients of characteristic eq.(14) are given by

$$\begin{aligned}
\Lambda_{11} &= c_{55}\alpha^2 - c_{11}\xi^2 + \rho\omega^2 \\
\Lambda_{12} &= c_{45}\alpha^2 - c_{16}\xi^2 \\
\Lambda_{13} &= -j\xi\alpha(c_{13} + c_{55}) \\
\Lambda_{22} &= c_{44}\alpha^2 - c_{66}\xi^2 + \rho\omega^2 \\
\Lambda_{23} &= -j\xi\alpha(c_{36} + c_{45}) \\
\Lambda_{33} &= c_{33}\alpha^2 - c_{55}\xi^2 + \rho\omega^2
\end{aligned} \tag{A.1}$$

$$A_1 = c_{33}c_{45}^2 - c_{33}c_{44}c_{55}$$

$$
\begin{aligned}
A_2 &= [c_{11}c_{33}c_{44} + c_{55}F_1 - c_{16}c_{33}c_{45} - c_{45}F_2 + (c_{13}+c_{55})F_3]\xi^2 + \\
&\quad [c_{55}(c_{33}+c_{44}) + c_{33}c_{44} - c_{45}^2]\rho\omega \\
A_3 &= [(c_{13}+c_{55})F_4 + c_{45}c_{16}c_{55} + c_{16}F_2 - c_{55}^2c_{66} - c_{11}F_1]\xi^4 + \\
&\quad [(c_{13}+c_{55})^2 + 2c_{45}c_{16} - F_1 - c_{55}(c_{55}+c_{66}) - c_{11}(c_{33}+c_{44})]\rho\omega\xi^2 - \\
&\quad (c_{33}+c_{44}+c_{55})\rho^2\omega^2 \qquad \text{(A.2)} \\
A_4 &= (c_{11}c_{55}c_{66} - c_{16}^2c_{55})\xi^6 + [c_{11}(c_{55}+c_{66}-c_{16}^2]\rho\omega\xi^4 + \\
&\quad (c_{11}+c_{55}+c_{66})\rho^2\omega^2\xi^2 + \rho^3\omega^3
\end{aligned}
$$

$$
\begin{aligned}
F_1 &= c_{33}c_{66} + c_{44}c_{55} - (c_{36}+c_{45})^2 \\
F_2 &= c_{33}c_{16} + c_{45}c_{55} - (c_{36}+c_{45})(c_{13}+c_{55}) \\
F_3 &= c_{45}(c_{36}+c_{45}) - c_{44}(c_{13}+c_{55}) \qquad \text{(A.3)} \\
F_4 &= c_{66}(c_{13}+c_{55}) - c_{16}(c_{36}+c_{45})
\end{aligned}
$$

Appendix B:

Various coefficients of eq.(32-40) are given by

$$
\begin{aligned}
G_{11} &= D_{23}D_{35} - D_{33}D_{25} \\
G_{21} &= D_{13}D_{35} - D_{33}D_{15} \\
G_{31} &= D_{13}D_{25} - D_{15}D_{23} \\
G_{13} &= D_{31}D_{25} - D_{21}D_{35} \\
G_{23} &= D_{31}D_{15} - D_{11}D_{35} \qquad \text{(B.1)} \\
G_{33} &= D_{15}D_{21} - D_{11}D_{25} \\
G_{15} &= D_{21}D_{33} - D_{31}D_{23} \\
G_{25} &= D_{11}D_{33} - D_{31}D_{13} \\
G_{35} &= D_{11}D_{23} - D_{13}D_{21}
\end{aligned}
$$

$$
H_{11} = D_{15}D_{23}\coth(\alpha_5 d) - D_{13}D_{25}\coth(\alpha_3 d)
$$

$$
\begin{aligned}
H_{12} &= D_{15}D_{33}\coth(\alpha_5 d) - D_{13}D_{35}\coth(\alpha_3 d) \\
H_{21} &= D_{15}D_{21}\coth(\alpha_5 d) - D_{11}D_{25}\coth(\alpha_1 d) \\
H_{22} &= D_{15}D_{31}\coth(\alpha_5 d) - D_{11}D_{35}\coth(\alpha_1 d) \\
H_{31} &= D_{13}D_{21}\coth(\alpha_3 d) - D_{11}D_{23}\coth(\alpha_1 d) \\
H_{32} &= D_{13}D_{31}\coth(\alpha_3 d) - D_{11}D_{33}\coth(\alpha_1 d) \\
H_{41} &= D_{15}D_{23}\coth(\alpha_3 d) - D_{13}D_{25}\coth(\alpha_5 d) \\
H_{42} &= D_{15}D_{33}\coth(\alpha_3 d) - D_{13}D_{35}\coth(\alpha_5 d) \\
H_{51} &= D_{15}D_{21}\coth(\alpha_1 d) - D_{11}D_{25}\coth(\alpha_5 d) \\
H_{52} &= D_{15}D_{31}\coth(\alpha_1 d) - D_{11}D_{35}\coth(\alpha_5 d) \\
H_{61} &= D_{13}D_{21}\coth(\alpha_1 d) - D_{11}D_{23}\coth(\alpha_3 d) \\
H_{62} &= D_{13}D_{31}\coth(\alpha_1 d) - D_{11}D_{33}\coth(\alpha_3 d)
\end{aligned}
\tag{B.2}
$$

and

$$
\begin{aligned}
R_{11} &= (R_3 - R_6)D_{15}\coth(\alpha_5 d) - (R_1 + R_4)D_{35} \\
R_{22} &= (R_2 - R_5)D_{15}\coth(\alpha_5 d) - (R_1 + R_4)D_{25} \\
R_{33} &= (R_1 - R_4)D_{35}\coth(\alpha_5 d) - (R_3 + R_6)D_{15} \\
R_{44} &= (R_1 - R_4)D_{25}\coth(\alpha_5 d) - (R_2 + R_5)D_{15} \\
R_{55} &= (R_3 - R_6)D_{13}\coth(\alpha_3 d) - (R_1 + R_4)D_{33} \\
R_{66} &= (R_2 - R_5)D_{13}\coth(\alpha_3 d) - (R_1 + R_4)D_{23} \\
R_{77} &= (R_1 - R_4)D_{33}\coth(\alpha_3 d) - (R_3 + R_6)D_{13} \\
R_{88} &= (R_1 - R_4)D_{23}\coth(\alpha_3 d) - (R_2 + R_5)D_{13}
\end{aligned}
\tag{B.3}
$$

Chapter 2

WAVE PROPAGATION IN ANISOTROPIC MEDIA DUE TO TRANSIENT SOURCES

2.1 Introduction

Plane harmonic wave interaction with homogeneous elastic anisotropic media, in general, and with layered anisotropic media, in particular, have been extensively investigated in the past decade or so. This advancement has been prompted, at least from a mechanics point of view, by the increased use of advanced composite materials in many structural applications. Being both anisotropic and dispersive, composite materials required in depth understanding of their mechanical behavior. The list of relevant literature is rather long and we thus refer the reader to selective recent works for further references [1-6].

The difficulties inherent in the treatment of wave propagation in anisotropic media in general can be illustrated by considering slowness wave surface methods for infinite media [1,7-9]. In this analysis, the slowness surface of an isotropic material consists of two concentric spherical sheets, an inner one rep-

resenting the longitudinal wave mode and an outer one representing the two degenerate transverse modes. In the anisotropic case, we find three general wave surfaces, one for the so-called quasi-longitudinal wave and two nondegenerate sheets for the quasi-transverse waves. Moreover, the surfaces will no longer be spherical in shape but will reflect the elastic symmetry or asymmetry of the material.

Perhaps the most severe consequence of elastic anisotropy in infinite media is the loss of pure wave modes for general propagation directions. This fact also implies that the direction of energy flow (i.e., group velocity) does not generally coincide with the wave vector, or wavefront normal. Thus, uncoupled pure potentials (such as are found in the isotropic case) are much easier to treat than the mixed modes characteristic of anisotropic materials. For wave propagation in directions of symmetry some wave types revert to pure modes, leading to a simpler characteristic equation of lower order.

A key condition which was found to facilitate the previous analysis is that at any boundary all wave vectors must lie in the same plane. This requirement implies that the response of the media will be independent of the in-plane coordinate normal to the propagation direction. Accordingly the analysis was conducted in a coordinate system formed by the line load direction and its normals rather than one determined by material symmetry axes. This choice leads to a significant simplification in algebraic analysis and computations.

In comparision to the extensive literature on the interaction of plane harmonic waves with anisotropic media, very little work is available on the response of such media to concentrated source loading. Here concentrated sources include point as well as line loads of which harmonically pulsating and transient sources are common types of such loading. Understanding the response of elastic solids to internal mechanical sources has long been of interest

to researchers in classical fields such as acoustics, seismology, as well as modern fields of application like ultrasonics and acoustic emission. It is known that whenever a material undergoes a local failure, elastic waves are generated due to the rapid release of localized strain energy. Such radiation, for example, is known as acoustic emission in the field of nondestructive testing of materials. In seismology it is of course known as earthquake.

A quick review of available literature on this subject reveals that most of the work done so far is carried out on isotropic media. The effect of imposed line load in homogeneous isotropic media has been discussed by several investigators ever since Lord Rayleigh discovered the existence of surface waves on the surfaces of solids [10]. An account of the literature dealing with this problem through 1957 can be found in Ewing, Jardetsky and Press [18]. Most of the earlier work [13-15] followed Lamb [11,12], who apparently was the first to consider the motion of semi-infinite space caused by a vertically applied line load on the free surface or within the medium. It was shown that displacements at large distance consists of a series of events which corresponds to the arrival of longitudinal, shear, and Rayleigh surface wave. The analytical approach used in the above mentioned investigations and others [13-15] can be summarized as follows : The steady state problem for harmonically pulsating source in infinite isotropic media is solved at first and then generalized to the case of half-space using superposition technique. For transient source loading results can be obtained from those corresponding to harmonic ones by a Fourier integral approach. The resulting double integral could be evaluated only by considering large distances.

A modern alternative approach has been suggested by Cagniard [16]. He showed that a suitable deformation of the integral contour not only resulted in considerable analytical simplification but led to exact, closed form, algebraic

expressions for the displacements as functions of time. Subsequently, many investigators have obtained the disturbances due to sources in the isotropic media by applying Cargniard approach [17]. DeHoop simplified Cargniard's method considerably and applied to cases involving impulsive line and point sources in infinite homogeneous isotropic media [18-21]. Kraut(1963) applied the Cargniard-DeHoop method for investigating the transient disturbance caused by a surface line load in the anisotropic half-space. Van der Hijden(1987) investigated the features of the wave propagation in infinite anisotropic media generated by a mechanical line source [28].

In this paper, we closely follow the formal developments in previous works [1-6] and study the response of two anisotropic systems to transient buried line loads. This analysis include infinite and semi-infinite systems. The foregoing illustration shall be carried out on anisotropic media possessing monoclinic or higher symmetry. The load will be in the form of a normal stress load acting at an arbitrary direction in the plane of symmetry of the material. One then uses a building block approach in which one starts by driving results for an infinite media. Subsequently one obtains the results for the half-space employing superposition of the infinite medium solution together a scattered solution from the boundary. The sum of both solutions has to satisfy stress free boundary conditions thereby yielding to complete solutions. Consequently explicit solutions for the particle displacements in both systems are obtained using Cargniard-DeHoop contour.

This work will accomplished by using the linear transformation approach in which one identifies the line load with the x_2 direction. This implies that all involved field variables will be independent of the x_2 direction. Nevertheless, and in general, one has three nonvanishing particle displacements. Material systems of higher symmetry, such as orthotropic, transversely isotropic, cubic,

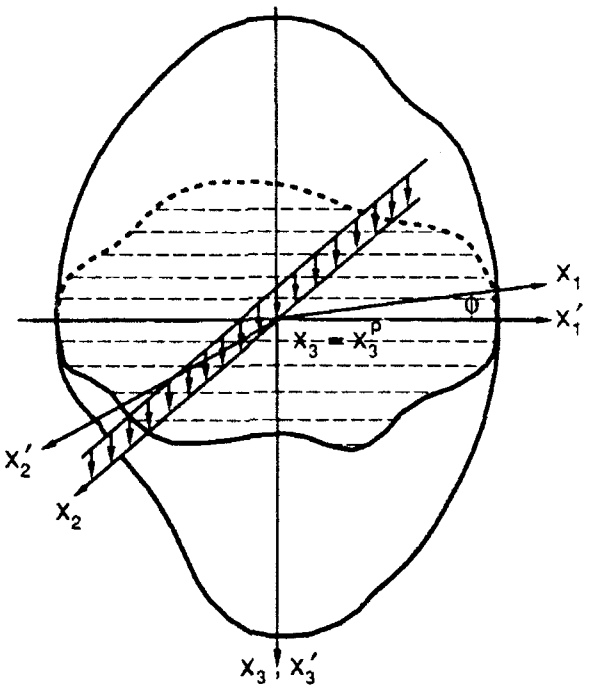

Figure 2.1: A applied line load in an anisotropic infinite media

and isotropic are contained implicitly in the analysis. Numerical results are demonstrated, drawn from concrete examples of materials belonging to several of these symmetry groups. It is found that for orthotropic and higher symmetry materials where the remaining two principal axes lie in the plane of symmetry, the particle motions in the sagittal and the normal to it uncouple if propagation occurs along either of these in-plane axes.

2.2 Theoretical development

Consider an infinite anisotropic elastic medium possessing monoclinic symmetry. The medium is oriented with respect to the reference cartesian coordinate system $x_i' = (x_1', x_2', x_3')$ such that the x_3' is assumed normal to its plane of symmetry as shown in figure 1. The plane of symmetry defining the mono-

clinic symmetry is thus coincident with the $x_1' - x_2'$ plane. With respect to this primed coordinate system, the equations of motion in the medium are given by [1]

$$\frac{\partial \sigma_{ij}'}{\partial x_j'} + f_i' = \rho' \frac{\partial^2 u_i'}{\partial t^2} \tag{2.1}$$

and, from the general constitutive relations for anisotropic media,

$$\sigma_{ij}' = c_{ijkl}' e_{kl}', \qquad i,j,k,l = 1,2,3 \tag{2.2}$$

by the specialized expanded matrix form to monoclinic media

$$\begin{pmatrix} \sigma_{11}' \\ \sigma_{22}' \\ \sigma_{33}' \\ \sigma_{23}' \\ \sigma_{13}' \\ \sigma_{12}' \end{pmatrix} = \begin{pmatrix} c_{11}' & c_{12}' & c_{13}' & 0 & 0 & c_{16}' \\ c_{12}' & c_{22}' & c_{23}' & 0 & 0 & c_{26}' \\ c_{13}' & c_{23}' & c_{33}' & 0 & 0 & c_{36}' \\ 0 & 0 & 0 & c_{44}' & c_{45}' & 0 \\ 0 & 0 & 0 & c_{45}' & c_{55}' & 0 \\ c_{16}' & c_{26}' & c_{36}' & 0 & 0 & c_{66}' \end{pmatrix} \begin{pmatrix} e_{11}' \\ e_{22}' \\ e_{33}' \\ \gamma_{23}' \\ \gamma_{13}' \\ \gamma_{12}' \end{pmatrix} \tag{2.3}$$

where the standard contracted subscript notations $1 \rightarrow 11$, $2 \rightarrow 22$, $3 \rightarrow 33$, $4 \rightarrow 23$, $5 \rightarrow 13$, and $6 \rightarrow 12$, to replace $c_{ijkl}(i,j,k,l = 1,2,3)$ with $c_{pq}(p,q = 1,2,...,6)$ are employed. Here σ_{ij}', e_{ij}' and u_i' are the components of stress, strain and displacement, respectively, and ρ' is the material density. In Eq.(1.3), $\gamma_{ij} = 2e_{ij}$ (with $i \neq j$) define the engineering shear strain components.

In what follows, one considers the response of the infinite medium to a uniform transient (time dependent) line load applied along a direction that makes an arbitrary azimuthal angle ϕ with the x_1' axis. That is, the direction $\phi = 0°$ coincides with the reference coordinate x_1'. Since, as was pointed out in the introduction, the response of the medium to such a wave is independent of the applied line direction. The analysis is conducted in a transformed coordinate system $x_i = (x_1, x_2, x_3)$ formed by a rotation of the plane $x_1' - x_2'$ through the angle ϕ about the x_3' direction. For convenience the direction x_2 is chosen to coincide with the line load direction.

Since c_{ijkl} is a fourth order tensor, then for any orthogonal transformation of the primed to the non-primed coordinates it transforms according to

$$c_{ijkl} = \beta_{im}\beta_{jn}\beta_{ko}\beta_{lp}c'_{mnop} \tag{2.4}$$

where β_{ij} is the cosine of the angle between x'_i and x_i. For a rotation of angle ϕ in the $x'_1 - x'_2$ plane, the transformation tensor β_{ij} reduces to

$$\beta_{ij} = \begin{bmatrix} \cos\phi & \sin\phi & 0 \\ -\sin\phi & \cos\phi & 0 \\ 0 & 0 & 1 \end{bmatrix} \tag{2.5}$$

If the transformation (1.5) is applied to Eq.(1.3), one obtains

$$\begin{pmatrix} \sigma_{11} \\ \sigma_{22} \\ \sigma_{33} \\ \sigma_{23} \\ \sigma_{13} \\ \sigma_{12} \end{pmatrix} = \begin{pmatrix} c_{11} & c_{12} & c_{13} & 0 & 0 & c_{16} \\ c_{12} & c_{22} & c_{23} & 0 & 0 & c_{26} \\ c_{13} & c_{23} & c_{33} & 0 & 0 & c_{36} \\ 0 & 0 & 0 & c_{44} & c_{45} & 0 \\ 0 & 0 & 0 & c_{45} & c_{55} & 0 \\ c_{16} & c_{26} & c_{36} & 0 & 0 & c_{66} \end{pmatrix} \begin{pmatrix} \epsilon_{11} \\ \epsilon_{22} \\ \epsilon_{33} \\ \gamma_{23} \\ \gamma_{13} \\ \gamma_{12} \end{pmatrix} \tag{2.6}$$

where the relations between the c_{pq} and c'_{pq} entries are listed in [5]. Notice that, no matter what rotational angle ϕ is used, the zero entries in Eq.(1.3) will remain zero in Eq.(1.6). In terms of the rotated coordinate system x_k, momentum equations can be written in the form

$$\frac{\partial \sigma_{ij}}{\partial x_j} + f_i = \rho \frac{\partial^2 u_i}{\partial t^2} \tag{2.7}$$

As mentioned earlier, in the rotated system, the elastic wave equations, for wave propagating in the $x_1 - x_3$ plane, are independent of x_2 . Nevertheless, the particle motion can generally have three nonzero components u_1, u_2, and u_3. The u_2 displacement can be identified as belonging to the horizontally polarized (SH) wave. Here, the equations describing these three wave motions are coupled in accordance with

$$[c_{11}\frac{\partial^2}{\partial x_1^2} + c_{55}\frac{\partial^2}{\partial x_3^2}]u_1 + [c_{16}\frac{\partial^2}{\partial x_1^2} + c_{45}\frac{\partial^2}{\partial x_3^2}]u_2$$

$$+\frac{\partial}{\partial x_3}[(c_{13}+c_{55})\frac{\partial}{\partial x_1}]u_3 = \rho\frac{\partial^2 u_1}{\partial t^2} - f_1 \quad (8a)$$

$$[c_{16}\frac{\partial^2}{\partial x_1^2}+c_{45}\frac{\partial^2}{\partial x_3^2}]u_1+[c_{66}\frac{\partial^2}{\partial x_1^2}+c_{44}\frac{\partial^2}{\partial x_3^2}]u_2$$
$$+\frac{\partial}{\partial x_3}[(c_{36}+c_{45})\frac{\partial}{\partial x_1}]u_3 = \rho\frac{\partial^2 u_2}{\partial t^2} - f_2 \quad (8b)$$

$$\frac{\partial}{\partial x_3}[(c_{13}+c_{55})\frac{\partial}{\partial x_1}]u_1+\frac{\partial}{\partial x_3}[(c_{36}+c_{45})\frac{\partial}{\partial x_2}]u_2$$
$$+[c_{55}\frac{\partial^2}{\partial x_1^2}+c_{33}\frac{\partial^2}{\partial x_3^2}]u_3 = \rho\frac{\partial^2 u_3}{\partial t^2} - f_3 \quad (8c)$$

f_i is chosen to be of the form

$$f_i = Q_i\delta(x_1)\delta(x_3 - x_3^p)F(t) \quad (2.9)$$

2.3 Source characterization

Using the above geometric arrangement, one describes the dirc delta line load as body force function located at the arbitrary location ($x_3 = x_3^p$). This choice of source location is arbitrary and is not necessary fcr the cases of propagation in either the infinite nor the semi-infinite media. However, as will be demonstrated, this choice will lead to great simplification in the algebraic manipulation for the propagation in the plate. Solutions to the present problem can be accomplished by following the procedure used by Achenbach [32]. According to this procedure, the infinite space can be thought of as consisting of two semi-spaces whose artificial interface contains the applied load. Thus the upper half-space occupies the region $x_3 \geq x_3^p$ whereas the lower half-space occupies the region $x_3 \leq x_3^p$. As a result of this, appropriate condition must be specified at the artificial interface.

In order to be able to specify these interface conditions, consider a very thin "interface" layer extending from $x_3 = x_3^p - o$ to $x_3 = x_3^p + o$; Then

start by requiring continuity on the displacement components and their time derivatives, namely

$$u_i(x_1, x_3, t)|_{x_3^p-o}^{x_3^p+o} = 0 \tag{10a}$$

$$\frac{\partial^{(n)} u_i(x_1, x_3, t)}{\partial t^{(n)}}|_{x_3^p-o}^{x_3^p+o} = 0, \quad i = 1, 2, 3 \tag{10b}$$

Integrating Eqs.(8a,b,c) across the interface layer and using the continuity equations(10a,b), leads to the discontinuity in the displacement spatial derivatives resulting in the following jump conditions.

$$(c_{55}\frac{\partial u_1}{\partial x_3} + c_{45}\frac{\partial u_2}{\partial x_3})|_{x_3^p-o}^{x_3^p+o} = -Q_1\delta(x_1)F(t) \tag{11a}$$

$$(c_{45}\frac{\partial u_1}{\partial x_3} + c_{44}\frac{\partial u_2}{\partial x_3})|_{x_3^p-o}^{x_3^p+o} = -Q_2\delta(x_1)F(t) \tag{11b}$$

$$c_{33}\frac{\partial u_3}{\partial x_3}|_{x_3^p-o}^{x_3^p+o} = -Q_3\delta(x_1)F(t) \tag{11c}$$

Now, consider the special case where $Q_1 = Q_2 = 0$ and $Q_3 = Q$. For this situation equations (11) reduce to.

$$(c_{55}\frac{\partial u_1}{\partial x_3} + c_{45}\frac{\partial u_2}{\partial x_3})|_{x_3^p-o}^{x_3^p+o} = 0 \tag{12a}$$

$$(c_{45}\frac{\partial u_1}{\partial x_3} + c_{44}\frac{\partial u_2}{\partial x_3})|_{x_3^p-o}^{x_3^p+o} = 0 \tag{12b}$$

$$c_{33}\frac{\partial u_3}{\partial x_3}|_{x_3^p-o}^{x_3^p+o} = \sigma_{33}|_{x_3^p-o}^{x_3^p+o} = -Q\delta(x_1)F(t) \tag{12c}$$

Examination of the relations (12a,b) reveals that, if $(c_{44}c_{55} - c_{45}^2)$ does not vanish (which is the case), then u_1 and u_2 must be at least constant and, in accordance with (10), equal. This constant is then chosen to be zero and thus conclude that u_1 and u_2 vanish at the interface. Finally, satisfing the normal stress discontinuity condition (13c) and assigning

$$c_{33}\frac{\partial u_3}{\partial x_3}|_{x_3^p+o} = -Q\delta(x_1)F(t)/2, \quad c_{33}\frac{\partial u_3}{\partial x_3}|_{x_3^p-o} = Q\delta(x_1)F(t)/2 \tag{2.13}$$

Collecting the above conditions one can summarize the condition at the artificial interface as

$$\left.\begin{array}{l} u_1 = 0 \\ u_2 = 0 \\ c_{33}\dfrac{\partial u_3}{\partial x_3} = -\dfrac{1}{2}Q\delta(x_1)F(t) \end{array}\right\}, \qquad \text{for } x_3 \geq x_3^p \text{ at } x_3 = x_3^p \tag{2.14}$$

$$\left.\begin{array}{l} u_1 = 0 \\ u_2 = 0 \\ c_{33}\dfrac{\partial u_3}{\partial x_3} = \dfrac{1}{2}Q\delta(x_1)F(t) \end{array}\right\}, \qquad \text{for } x_3 \leq x_3^p \text{ at } x_3 = x_3^p \tag{2.15}$$

2.4 Integral transforms of formal solutions

Following the procedure of [1], let us outline the steps leading to a formal solutions of Eqs.(8a,b,c) for each of the two semi-spaces. Since the body force has been replaced by the "artificial interface" condition, one can drop f_i from Eqs(8a,b,c). Assume formal solutions followed by applying the Fourier transform to these equations in accordance with

$$\bar{u}_i = \int_0^\infty u_i e^{-pt} dt \tag{2.16}$$

$$\hat{u}_i = \int_{-\infty}^\infty \bar{u}_i e^{-jp\eta x_1} dx_1 \tag{2.17}$$

The general solution of the resulting differential equations is then sought in the form

$$\hat{u}_i = U_i e^{-p\alpha x_3}, \quad i = 1,2,3 \tag{2.18}$$

leading to the characteristic equation

$$\begin{pmatrix} \Lambda_{11} & \Lambda_{12} & \Lambda_{13} \\ \Lambda_{12} & \Lambda_{22} & \Lambda_{23} \\ \Lambda_{13} & \Lambda_{23} & \Lambda_{33} \end{pmatrix} \begin{pmatrix} U_1 \\ U_2 \\ U_3 \end{pmatrix} = 0 \tag{2.19}$$

where the various entries Λ_{ij} are given in Appendix A. Note from (1.19) that the Λ_{ij} matrix is symmetric.

For the existence of nontrivial solutions in U_i the determinant in Eq. (1.19), must vanish giving an algebraic equation of α. This is an alternative presentation of Christoffel equation [2]. The difference is that one now solves for α as compared with solving for the phase velocity for a given propagation direction. Upon setting the determinant equal to zero, one obtains a sixth order equation in α (cubic in α^2) which is written symbolically as

$$A_1\alpha^6 + A_2\alpha^4 + A_3\alpha^2 + A_4 = 0 \tag{2.20}$$

with its coefficients are given in Appendix B. Eq.(1.20) admits six solutions for α. These α's have the further properties that

$$\alpha_2 = -\alpha_1,\ \alpha_4 = -\alpha_3,\ \alpha_6 = -\alpha_5 \tag{2.21}$$

Furthermore for each α, equation(18) yields the displacement amplitude ratios $v_q = U_{2q}/U_{1q}, w_q = U_{3q}/U_{1q}$

$$v_q = -\frac{\Lambda_{11}\Lambda_{23} - \Lambda_{12}\Lambda_{13}}{\Lambda_{12}\Lambda_{23} - \Lambda_{22}\Lambda_{13}} \tag{21a}$$

$$w_q = -\frac{\Lambda_{12}\Lambda_{23} - \Lambda_{13}\Lambda_{22}}{\Lambda_{23}\Lambda_{23} - \Lambda_{22}\Lambda_{33}} \tag{21b}$$

Finally, invoking superposition, one can write the formal solutions for the displacements of equations (8a,b,c) and their associated stress components using Eq.(1.6) as

$$(\hat{u}_1, \hat{u}_2, \hat{u}_3) = \sum_{q=1}^{6}(1, v_q, w_q)U_{1q}e^{-p\alpha_q(x_3 - x_3^p)} \tag{2.22}$$

$$(\hat{\sigma}_{33}, \hat{\sigma}_{13}, \hat{\sigma}_{23}) = \sum_{q=1}^{6} p(D_{1q}, D_{2q}, D_{3q})U_{1q}e^{-p\alpha_q(x_3 - x_3^p)} \tag{2.23}$$

where

$$D_{1q} = j\eta(c_{13} + c_{36}v_q) - c_{33}\alpha_q w_q \tag{2.24}$$

$$D_{2q} = c_{55}(j\eta w_q - \alpha_q) - c_{45}\alpha_q v_q \tag{2.25}$$

$$D_{3q} = c_{45}(j\eta w_q - \alpha_q) - c_{44}\alpha_q v_q, \qquad q = 1, 2, .., 6 \tag{2.26}$$

With reference to equation the relation (20) and to the Λ_{ij} entries of Appendix A and by inspection of equations (20) and (24-26), one recognizes the relations (see Ref.[2])

$$\begin{array}{llllll} v_2 & = v_1, & v_4 & = v_3, & v_6 & = v_5 \\ w_2 & = -w_1, & w_4 & = -w_3, & w_6 & = -w_5 \\ D_{12} & = D_{11}, & D_{14} & = D_{13}, & D_{16} & = D_{15} \\ D_{22} & = -D_{21}, & D_{24} & = -D_{23}, & D_{26} & = -D_{25} \\ D_{32} & = -D_{31}, & D_{34} & = -D_{33}, & D_{36} & = -D_{35} \end{array} \tag{2.27}$$

The above solutions with their various properties can now be specialized to both artificial half-spaces by the following steps. Inspection of the above solutions indicate that each consists of three pairs of wave components, each pair propagating in mirror image fashion with respect to the interface, namely along positive and negative x_3-directions. Since propagation is expected to emanate from the interface into both media, we arbitrary reserve q_1, q_3, and q_5 for the lower half-space; the remaining one's, namely described with q_2, q_4, and q_6 for the upper one. We list the formal solution in the lower and lower half-spaces according to

$$\left.\begin{array}{l} (\hat{u}_1, \hat{u}_2, \hat{u}_3) = \sum\limits_{q=1,3,5} (1, v_q, w_q) U_{1q} e^{-p\alpha_q(x_3 - x_3^p)} \\ (\hat{\sigma}_{33}, \hat{\sigma}_{13}, \hat{\sigma}_{23}) = \sum\limits_{q=1,3,5} p(D_{1q}, D_{2q}, D_{3q}) U_{1q} e^{-p\alpha_q(x_3 - x_3^p)} \end{array}\right\} \; x_3 \geq x_3^p \tag{2.28}$$

$$\left.\begin{array}{l} (\hat{u}_1, \hat{u}_2\ \hat{u}_3) = \sum\limits_{q=2,4,6} (1, v_q, w_q) U_{1q} e^{-p\alpha_q(x_3 - x_3^p)} \\ (\hat{\sigma}_{33}, \hat{\sigma}_{13}, \hat{\sigma}_{23}) = \sum\limits_{q=2,4,6} p(D_{1q}, D_{2q}, D_{3q}) U_{1q} e^{-p\alpha_q(x_3 - x_3^p)} \end{array}\right\} \; x_3 \leq x_3^p \tag{2.29}$$

Specialization of formal solutions to infinite media

At this point, a formal solution of the field equation in a monoclinic medium has been presented. The amplitudes U_{1q} are the unknowns. The amplitudes U_{1q} will now be determined by implementing the artificial interface conditions (1.14-1.15). To this end, if (28) is subjected to the conditions (14) and (29) to (15), one finally solves the displacement amplitudes as

$$U_{11} = -U_{12} = (v_5 - v_3)\bar{F}(p)Q/(2c_{33}D_{um}p) \tag{30a}$$

$$U_{13} = -U_{14} = (v_1 - v_5)\bar{F}(p)Q/(2c_{33}D_{um}p) \tag{30b}$$

$$U_{15} = -U_{16} = (v_3 - v_1)\bar{F}(p)Q/(2c_{33}D_{um}p) \tag{30c}$$

where

$$D_{um} = v_1(\alpha_3 w_3 - \alpha_5 w_5) + v_3(\alpha_5 w_5 - \alpha_1 w_1) + v_5(\alpha_1 w_1 - \alpha_3 w_3) \tag{2.31}$$

It is interesting to note that $D_{um} = 0$ defines an equivalent Christoffel characteristic equation for the propagation of bulk waves in the medium. With these solutions for the wave amplitudes, solutions in the upper region can be written in terms of $q = 1, 3, 5$ as

$$\begin{aligned}(\hat{u}_1, \hat{u}_2, \hat{u}_3) &= \sum_{q=1,3,5} (-1, -v_q, w_q)U_{1q}e^{-p\alpha_q(x_3^p - x_3)} \\ (\hat{\sigma}_{33}, \hat{\sigma}_{13}, \hat{\sigma}_{23}) &= \sum_{q=1,3,5} p(-D_{1q}, D_{2q}, D_{3q})U_{1q}e^{-p\alpha_q(x_3^p - x_3)}\end{aligned} \tag{2.32}$$

In summary, solutions (28) and (32) with the amplitude solutions (30) uniquely define the propagation fields in the lower and upper "artificial" semi-spaces. In other words, their combination constitute the total solutions for the infinite medium.

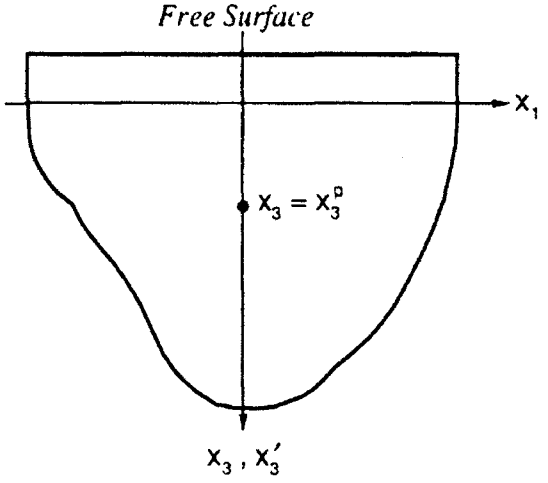

Figure 2.2: Semi-infinite media

Specialization of formal solutions to half-spaces

One now adapts the solutions of the infinite media (2.28) and (2.32) for solution of the case where the free boundary is intercepts the propagating waves at some arbitrary location parallel to the plane $x_3 = 0$. Assuming that the free boundary is located at $x_3 = -d$ as depicted in figure 2. The implication is that the free boundary is located in the upper region and thus can only interfere with the propagation fields in the negative x_3 direction. For this case, the solution (2.32) will constitute an incident wave on free surface. As a results waves will reflect from the free boundary and propagate in the positive x_3 direction. Thus, appropriate formal solutions for the reflected waves can be adapted from the solution (2.28) in accordance with (Note now that x_3^p does not appear because solutions are referred to the origin $x_3 = 0$)

$$(\hat{u}_1^r, \hat{u}_2^r, \hat{u}_3^r) = \sum_{q=1,3,5} (1, v_q, w_q) U_{1q}^r e^{-p\alpha_q x_3} \tag{2.33}$$

$$(\hat{\sigma}_{33}^r, \hat{\sigma}_{13}^r, \hat{\sigma}_{23}^r) = \sum_{q=1,3,5} p(D_{1q}, D_{2q}, D_{3q}) U_{1q}^r e^{-p\alpha_q x_3} \tag{2.34}$$

With this the total solution for the semi-space (designated with superscript 's') which is required to satisfy the stress free boundary condition is obtained by superposing the incident waves and reflected waves in accordance with

$$\begin{aligned}(\hat{u}_1^s, \hat{u}_2^s, \hat{u}_3^s) &= \sum_{q=1,3,5} (-1, -v_q, w_q) U_{1q}^{(i)} e^{-p\alpha_q(x_3^p - x_3)} \\ &+ \sum_{q=1,3,5} (1, v_q, w_q) U_{1q}^r e^{-p\alpha_q x_3}\end{aligned} \tag{2.35}$$

$$\begin{aligned}(\hat{\sigma}_{33}^s, \hat{\sigma}_{13}^s, \hat{\sigma}_{23}^s) &= \sum_{q=1,3,5} p(-D_{1q}, D_{2q}, D_{3q}) U_{1q}^{(i)} e^{-p\alpha_q(x_3^p - x_3)} \\ &+ \sum_{q=1,3,5} p(D_{1q}, D_{2q}, D_{3q}) U_{1q}^r e^{-p\alpha_q x_3}\end{aligned} \tag{2.36}$$

The boundary condition is given by

$$\hat{\sigma}13^s = \hat{\sigma}23^s = \hat{\sigma}33^s = 0, \quad \text{at } x_3 = -d \tag{2.37}$$

By imposing the boundary conditions (2.37) on Eq.(6), linear system is obtained by

$$\begin{pmatrix} D_{11} & D_{13} & D_{15} \\ D_{21} & D_{23} & D_{25} \\ D_{31} & D_{33} & D_{35} \end{pmatrix} \begin{pmatrix} U_{11}^r E_1 \\ U_{13}^r E_3 \\ U_{15}^r E_5 \end{pmatrix} = \begin{pmatrix} R_1 \\ R_3 \\ R_5 \end{pmatrix} \tag{2.38}$$

where

$$R_1 = -(U_{11}^{(i)} D_{11} E_1^r + U_{13}^{(i)} D_{13} E_3^r + U_{15}^{(i)} D_{15} E_5^r) \tag{39a}$$

$$R_3 = (U_{11}^{(i)} D_{21} E_1^r + U_{13}^{(i)} D_{23} E_3^r + U_{15}^{(i)} D_{25} E_5^r) \tag{39b}$$

$$R_5 = (U_{11}^{(i)} D_{31} E_1^r + U_{13}^{(i)} D_{33} E_3^r + U_{15}^{(i)} D_{35} E_5^r) \tag{39c}$$

Using Cramer's rule solve for the reflected amplitudes obtaining

$$U_{11}^r = \frac{1}{D_{sm} E_1} (R_1 G_{11} - R_3 G_{21} + R_5 G_{31}) \tag{40a}$$

$$U_{13}^r = \frac{-1}{D_{sm} E_3} (R_1 G_{13} - R_3 G_{23} + R_5 G_{33}) \tag{40b}$$

$$U_{15}^r = \frac{1}{D_{sm}E_5}(R_1G_{15} - R_3G_{25} + R_5G_{35}) \tag{40c}$$

with

$$E_q = e^{p\alpha_q d}, E_q^r = e^{-p\alpha_q(x_3^p+d)}, \qquad \text{q=1.3.5} \tag{2.41}$$

and

$$D_{sm} = D_{11}G_{11} - D_{21}G_{21} + D_{31}G_{31} \tag{2.42}$$

Where the G_{qr} are given in Appendix B. Note that $D_{sm} = 0$ defines the characteristic equations for the propagation of Rayleigh (surface) wave on the free surface [1]

2.5 Cargniard-DeHooop contour variation

Infinite media

Now consider the transformations back to the time-space domain using Cargniard DeHoop method. Choose F(t) as the delta function $\delta(t)$ Laplace transform of which is equal to 1. Then, consider the Laplace transform of u_1. $\bar{u}_1$ is obtained by

$$\begin{aligned} 2\pi\bar{u}_1 = & \int_{-\infty}^{\infty} U_{11}e^{-p(\alpha_1 x_3 - j\eta x_1)}d\eta + \int_{-\infty}^{\infty} U_{13}e^{-p(\alpha_3 x_3 - j\eta x_1)}d\eta + \\ & \int_{-\infty}^{\infty} U_{15}e^{-p(\alpha_5 x_3 - j\eta x_1)}d\eta \end{aligned} \tag{2.43}$$

Since, next one wishes to carry out the integration with respect to η along a certain contour in the complex η-plane that deviates from the positive imaginary axis, extend the definition of the relevant integral into the complex η-plane by analytic continuation away from the imaginary η-axis. This deformation of the integration contour is only valid if no singularities are crossed. One

can prove (Burridge 1970) that the only singularity in the η-plane are: (a) branch points on the imaginary axis where up- and down-going waves meet: (b) possible branch points off the imaginary axis where other two upgoing or downgoing waves meet; (c) poles on the imaginary axis to the lowermost point, and to the uppermost branch point (The present of poles is linked to the existence of interface waves at one or more of the interfaces that are present in the configuration; the poles do not occur in the case of an infinite homogeneous solid). The singularities of type (b) are no obstruction to the contour deformation process as long as summations of the contributions of the relevant three generalized rays are taken into account by adding the results from the three contour integrals. Thus, in the deformation process one only has to assure that one does not cross any of the branch points on the imaginary η-axis. Now, change the contour of the η integration from the positive imaginary axis in the complex η-plane to the Cargniard-DeHoop contour, parameterized by the real time-variable t running from t_q, the arrival time of a certain wave, to infinity. This integral can be recognized as the Laplace transforms of certain explicit functions of time, thus the inverse transforms by inspection as detailed in Achenbach[32]. The integration in the complex η-plane is carried out along the (in general, six different) paths where

$$t = \alpha x_3 - j\eta x_1 \tag{2.44}$$

with t real and positive. The paths that are traced by these different η as t increases are the Cargniard-DeHoop contour. The Cargniard-DeHoop method is based on the following elementary property of the one-sided Laplace transform: for given Laplace transforms,

$$\bar{u}_i = \int_{t_q}^{\infty} u_i(x_1, x_3, t) e^{-pt} dt \tag{2.45}$$

the inverse of the integral is exactly of the form of

$$u_i = u_i(x_1, x_3, t)H(t - tq) \tag{2.46}$$

where H(t-tq) is the Heavyside step function. Equation (2.44) is written with respect to α by

$$\alpha = \frac{t + j\eta x_1}{x_3} \tag{2.47}$$

Substitution of (2.46) into the characteristic equation (40) yields the sixth order polynomial defining the Fourier parameter η

$$\Omega(x_1, x_3, t, \eta) = 0 \tag{2.48}$$

where

$$\Omega(x_1, x_3, t, \eta) = B_6\eta^6 + B_5\eta^5 + B_4\eta^4 + B_3\eta^3 + B_2\eta^2 + B_1\eta + B_0 \tag{2.49}$$

The coefficient B_i is given in Appendix A. The distinct six roots of η are obtained from (2.47) with complex coefficients, which is the function of the spatial variables (x_1, x_3) and time (t). The six root of η is composed of three parabolas with respect to time t for a certain position (x_1, x_3), when they are plotted as real η versus imaginary η, and they are symmetric about the imaginary η axis. In the interesting range of time, the η curves form three branches. Each of the parabolas is associated with six distinct roots of α from the characteristic equation (20), three of which correspond to the lower half-space and others to the upper half-space, because of the boundedness of the waves. Each of the three η represents a separate wavefront.

Now the inverse Laplace transform can be obtained by mere inspection of (3.25)-(3.26) to be

$$\frac{4\pi c_{33}}{Q}u_1 = [\frac{(v_5 - v_3)}{D_{um}}(\eta_1^+)\frac{\partial \eta_1^+}{\partial t} - \frac{(v_5 - v_3)}{D_{um}}(\eta_1^-)\frac{\partial \eta_1^-}{\partial t}]H(t - t_1) +$$

$$[\frac{(v_1-v_5)}{D_{um}}(\eta_2^+)\frac{\partial\eta_2^+}{\partial t}-\frac{(v_1-v_5)}{D_{um}}(\eta_2^-)\frac{\partial\eta_2^-}{\partial t}]H(t-t_2)+$$
$$[\frac{(v_3-v_1)}{D_{um}}(\eta_3^+)\frac{\partial\eta_3^+}{\partial t}-\frac{(v_3-v_1)}{D_{um}}(\eta_3^-)\frac{\partial\eta_3^-}{\partial t}]H(t-t_3) \qquad (38a)$$

where t_1, t_2, and t_3 are the arrival times of the various wavefronts. In other words, they are the times that correspond to the values of the imaginary η-axis intercepts of the three branches of η. The notation η_i^+ denotes the branch of η_i to the right side of the imaginary η-axis and η_i^- denotes the branch of η_i to the left side of the imaginary η-axis. by using the same technique the displacement u_2 and u_3 are obtained by

$$\begin{aligned}
\frac{4\pi c_{33}}{Q}u_2 &= [\frac{(v_5-v_3)}{D_{um}}v_1(\eta_1^+)\frac{\partial\eta_1^+}{\partial t}-\frac{(v_5-v_3)}{D_{um}}v_1(\eta_1^-)\frac{\partial\eta_1^-}{\partial t}]H(t-t_1)+\\
&\quad [\frac{(v_1-v_5)}{D_{um}}v_3(\eta_2^+)\frac{\partial\eta_2^+}{\partial t}-\frac{(v_1-v_5)}{D_{um}}v_3(\eta_2^-)\frac{\partial\eta_2^-}{\partial t}]H(t-t_2)+\\
&\quad [\frac{(v_3-v_1)}{D_{um}}v_5(\eta_3^+)\frac{\partial\eta_3^+}{\partial t}-\frac{(v_3-v_1)}{D_{um}}v_5(\eta_3^-)\frac{\partial\eta_3^-}{\partial t}]H(t-t_3) \qquad (38b)\\
\frac{4\pi c_{33}}{Q}u_3 &= [\frac{(v_5-v_3)}{D_{um}}w_1(\eta_1^+)\frac{\partial\eta_1^+}{\partial t}-\frac{(v_5-v_3)}{D_{um}}w_1(\eta_1^-)\frac{\partial\eta_1^-}{\partial t}]H(t-t_1)+\\
&\quad [\frac{(v_1-v_5)}{D_{um}}w_3(\eta_2^+)\frac{\partial\eta_2^+}{\partial t}-\frac{(v_1-v_5)}{D_{um}}w_3(\eta_2^-)\frac{\partial\eta_2^-}{\partial t}]H(t-t_2)+\\
&\quad [\frac{(v_3-v_1)}{D_{um}}w_5(\eta_3^+)\frac{\partial\eta_3^+}{\partial t}-\frac{(v_3-v_1)}{D_{um}}w_5(\eta_3^-)\frac{\partial\eta_3^-}{\partial t}]H(t-t_3) \qquad (38c)
\end{aligned}$$

Half-space media

Employing the above procedure, integral transform solutions of Eq.(35) in the half-space are inversely transformed back to the space-time domain. However, It is impossible to consider the transient waves in the whole half-space by using Cagniard-DeHoop method, since the order of the exponential is the linear function of α_1, α_3, and α_5. Fortunately, one can investigate the surface

waves on the free surface, i.e., $x_3 = -d$. The reflected waves of Eq.(33) for the case of $x_3^p = 0$ and $x_3 = -d$ that is designated as superscript ^{rs} are simplified by

$$\begin{aligned}\frac{2c_{33}D_{um}D_{sm}}{QF}\hat{u}_{1m}^{rs} &= (v_5 - v_3)(D_{11}G_1^u - D_{21}G_2^u - D_{31}G_3^u)e^{-p\alpha_1 d} + \\ &\quad (v_1 - v_5)(D_{13}G_1^u - D_{23}G_2^u - D_{33}G_3^u)e^{-p\alpha_3 d} + \\ &\quad (v_3 - v_1)(D_{15}G_1^u - D_{25}G_2^u - D_{35}G_3^u)e^{-p\alpha_5 d} \qquad (2.50)\\ \frac{2c_{33}D_{um}D_{sm}}{QF}\hat{u}_{2m}^{rs} &= (v_5 - v_3)(D_{11}G_1^v + D_{21}G_2^v + D_{31}G_3^v)e^{-p\alpha_1 d} + \\ &\quad (v_1 - v_5)(D_{13}G_1^v + D_{23}G_2^v + D_{33}G_3^v)e^{-p\alpha_3 d} + \\ &\quad (v_3 - v_1)(D_{15}G_1^v + D_{25}G_2^v + D_{35}G_3^v)e^{-p\alpha_5 d} \qquad (2.51)\\ \frac{2c_{33}D_{um}D_{sm}}{QF}\hat{u}_{3m}^{rs} &= (v_5 - v_3)(D_{11}G_1^w - D_{21}G_2^w - D_{31}G_3^w)e^{-p\alpha_1 d} + \\ &\quad (v_1 - v_5)(D_{13}G_1^w - D_{23}G_2^w - D_{33}G_3^w)e^{-p\alpha_3 d} + \\ &\quad (v_3 - v_1)(D_{15}G_1^w - D_{25}G_2^w - D_{35}G_3^w)e^{-p\alpha_5 d} \qquad (2.52)\end{aligned}$$

with

$$G_r^u = \sum_{q=1}^{3} G_{qr}, \quad G_r^v = \sum_{q=1}^{3} G_{qr}u_q, \quad G_r^w = \sum_{q=1}^{3} G_{qr}w_q \qquad (2.53)$$

where G_{qr} is given in Appendix C. Now the particle displacements are obtained by superposing the incident waves on the free surface of Eq.(29) and reflected waves on the free surface of Eqs.(50-52). Now, the remaining task is to apply Cagniard-Dehoop method the same as infinite media. The result for u_1^s are given by

$$\frac{4\pi c_{33}}{Q}u_1^s =$$

$$\begin{aligned}&[\frac{(v_5 - v_3)}{D_{um}}(1 + (D_{11}G_1^u - D_{21}G_2^u - D_{31}G_3^u)/D_{sm})(\eta_1^+)\frac{\partial \eta_1^+}{\partial t} \\ &-\frac{(v_5 - v_3)}{D_{um}}(1 + (D_{11}G_1^u - D_{21}G_2^u - D_{31}G_3^u)/D_{sm})(\eta_1^-)\frac{\partial \eta_1^-}{\partial t}]H(t - t_1) +\end{aligned}$$

$$
\begin{aligned}
&[\frac{(v_1 - v_5)}{D_{um}}(1 + (D_{13}G_1^u - D_{23}G_2^u - D_{33}G_3^u)/D_{sm})(\eta_2^+)\frac{\partial \eta_2^+}{\partial t} \\
&-\frac{(v_1 - v_5)}{D_{um}}(1 + (D_{13}G_1^u - D_{23}G_2^u - D_{33}G_3^u)/D_{sm})(\eta_2^-)\frac{\partial \eta_2^-}{\partial t}]H(t - t_2) + \\
&[\frac{(v_3 - v_1)}{D_{um}}(1 + (D_{15}G_1^u - D_{25}G_2^u - D_{35}G_3^u)/D_{sm})(\eta_3^+)\frac{\partial \eta_3^+}{\partial t} \\
&-\frac{(v_3 - v_1)}{D_{um}}(1 + (D_{15}G_1^u - D_{25}G_2^u - D_{35}G_3^u)/D_{sm})(\eta_3^-)\frac{\partial \eta_3^-}{\partial t}]H(t - t_3) \quad (2.54)
\end{aligned}
$$

The remaining displacements u_2^s and u_3^s will be obtained by similiar procedures.

2.6 Numerical illustrations and discussions

In this section numerical illustrations of the above analysis are given. Let's choose for our illustration a cubic material. The microstructure of this particular material has been extensively studied and models predicting its effective anisotropic properties are available elsewhere [1]. The cubic material of InAs is given with respect to the reference coordinate system x_i' as

$$
c_{ij}' = \begin{pmatrix}
83.29 & 45.26 & 45.26 & 0 & 0 & 0 \\
45.26 & 83.29 & 45.26 & 0 & 0 & 0 \\
45.26 & 45.26 & 83.29 & 0 & 0 & 0 \\
0 & 0 & 0 & 39.59 & 0 & 0 \\
0 & 0 & 0 & 0 & 39.59 & 0 \\
0 & 0 & 0 & 0 & 0 & 39.59
\end{pmatrix} \times 10^{10} \quad [\ \mathrm{N/m^2}\ ]
$$

with $\rho = 5.67\ \mathrm{g/cm^3}$. For a rotation of $\phi = 30°$, for example, these properties transform to

$$
c_{ij}' = \begin{pmatrix}
51.20 & 36.28 & 4.03 & 0 & 0 & 36.13 \\
36.28 & 51.20 & 4.03 & 0 & 0 & 36.13 \\
4.03 & 4.03 & 16.00 & 0 & 0 & 0.31 \\
0 & 0 & 0 & 6.64 & 0 & 0 \\
0 & 0 & 0 & 0 & 6.64 & 0 \\
36.13 & 36.13 & 0.31 & 0 & 0 & 40.02
\end{pmatrix} \times 10^{10} \quad [\ \mathrm{N/m^2}\ ]
$$

which confirms the earlier conclusion that the transformed matrix takes the format of monoclinic symmetry. Having chosen the material let's summarize a "flow chart" like procedure for our subsequent calculations.

After specifying the azimuthal angle ϕ (namely, the line load direction) we proceed in the first step to evaluate η's from the sixth order polynomial (49) for given time and location (x_1, x_3). While time (t) is marching from 0, η's have three pairs of complex conjugates for $t \geq t_3$, two pairs of complex conjugates for $t_2 \leq t \leq t_3$, and a pair of complex conjugates for $t_1 \leq t \leq t_2$. t_q represents the arrival times of three kinds of wave. As the η doesn't have a pair of conjugate, displacements and stresses are equal to zero. The arrival times of three kinds of waves are collected with respect to arbitrary direction of wave propagation in $x_1 - x_3$ plane. The arrival times, the energy slowness, corresponding to arbitrary angle of ϕ for the cubic material are shown in figure 5-8. However, the cubic material has cuspidals in the plane of arrival time that represents lacunae, in which the elastic energy is zero. In the cuspidal, the material has as many as five arrival times. The number of arrival times, therefore, are dependent on materials. This agrees with [24]. The inverse of the plane of arrival time is the plane of the elastic energy, which shows the energy fronts of the wave propagation in the infinite media. Figure 5-8 shows the variation of energy front corresponding to azimuthal angle. This energy plane is exactly same as that calculated by the plane of slowness.

Next step is to solve the characteristic equation. One then has to decide which of the α_{ii} correspond to $\eta_i, i = 1, 3, 5$. If one determines the α_{ii} from α's that match with α of equation (27), the order of other two $\alpha_{ij}, i \neq j$ does not affect to the numerical results. The sign of $\mathrm{Re}(\alpha_{ij})$ follows sign of $\mathrm{Re}(\alpha_{ii})$, However, if the identification of the α's is in error, the final results of the displacements will clearly indicate that something is amiss. Lacking

the proper identification of the α's the calculated displacements will contain imaginary parts, a violation of the condition for the existence of the Laplace transform. Therefore, only the proper identification of the α's will yield purely real displacements so that the existence condition of the Laplace transform is satisfied. Of course once the existence condition is satisfied then the validity of the identification scheme was required since all of the explicit solutions for cubic equations "mixed" roots for the various of the parameter . Then the displacement ratios are calculated. Finally, displacements are determined by explicit solution of (31).

Response of infinite media

Numerical results for cubic medum of InAs with $\phi = 30°$ are shown in figure 3-4. Figure 3a shows the slowness curves and the direction of wave propagation 10° and 5°. Imaginary part of η variation with respect to time is shown in figure 3b or 4a. Thus designating t_1, t_2, t_3, t_4, and t_5 as the arrival times of various wave forms in order from figure figure 3b or 4a. The wave along the paths of η corresponding to $t_1 \leq t \leq t_2$ or $t \geq t_3$ represent quasi-longitudinal wave. The wave along a η of $t \geq t_4$ represent quasi-vertical shear wave. The wave along a η of $t \geq t_5$ represent quasi-horizontal shear wave. The time interval of $t_2 \leq t \leq t_3$ represents 'lacunae' that all the disturbances are zero.

Figures 5-8 show numerical illstrations corresponding to the azimuthal angle of the chosen several material systems : (a) variations of the energy flows, (b) energy slowness curves, and (c) displacement fields. In fact, the energy slowness curves show the arrival times for the various wave forms. Both energy (a) and energy slowness (b) curves are based on the slowness curves [7]. (c) present snap shots of absolute value of radical displacement field at fixed time (t = 0.2 microsec). A spatial grid of 100x100 points are

generated for the first quadrant. The remaining quadrants is then generated by the mirror of the first quadrant . The vertical line load is located at the origin. The origin is located at the center of the picture. Since the medium is homogeneous, the wave field does not change as it propagates. The color scheme runs from white (minimum) to black (maximum). In this picture we can clearly recognize the wave curves (three wave fronts and lacunae). This displacement intensity pictures agree with the energy flows (a).

The variations of the displacement fields corresponding to azimuthal angle for the cubic material of InAs are shown through figure 5-8. Very sharp displacement intensity and lacunae is presented in figure 5 in the cse of azimuthal angle $\phi = 0°$. As the azimuthal angle is increased by 10°, the third wave front, quasihorizontal shear wave is more clear and the lacunae disappears. We can not get the good numerical results arround 90° direction because of contour sigularity of integral (47).

Response of half-space media

In this section, numerical results in half-space media are discussed. The first case is to evaluate the response generated by an internal line load. One choosing for our illustration a cubic material of the perturbed steel, the material properties are given with respect to the reference coordinate system x_i' as

$$c_{ij}' = \begin{pmatrix} 278.74 & 33.00 & 33.00 & 0 & 0 & 0 \\ 33.00 & 278.74 & 33.00 & 0 & 0 & 0 \\ 33.00 & 33.00 & 278.74 & 0 & 0 & 0 \\ 0 & 0 & 0 & 81.91 & 0 & 0 \\ 0 & 0 & 0 & 0 & 81.91 & 0 \\ 0 & 0 & 0 & 0 & 0 & 81.91 \end{pmatrix} \times 10^{10} \quad [\ \mathrm{N/m^2}\ ]$$

with $\rho = 1.7\ \mathrm{g/cm^3}$. Figure 9 show a slowness curves (a) and displacements versus time, u_1 (b) and u_3 (c), for $\phi = 30°$. The receiver is located at (2.0,

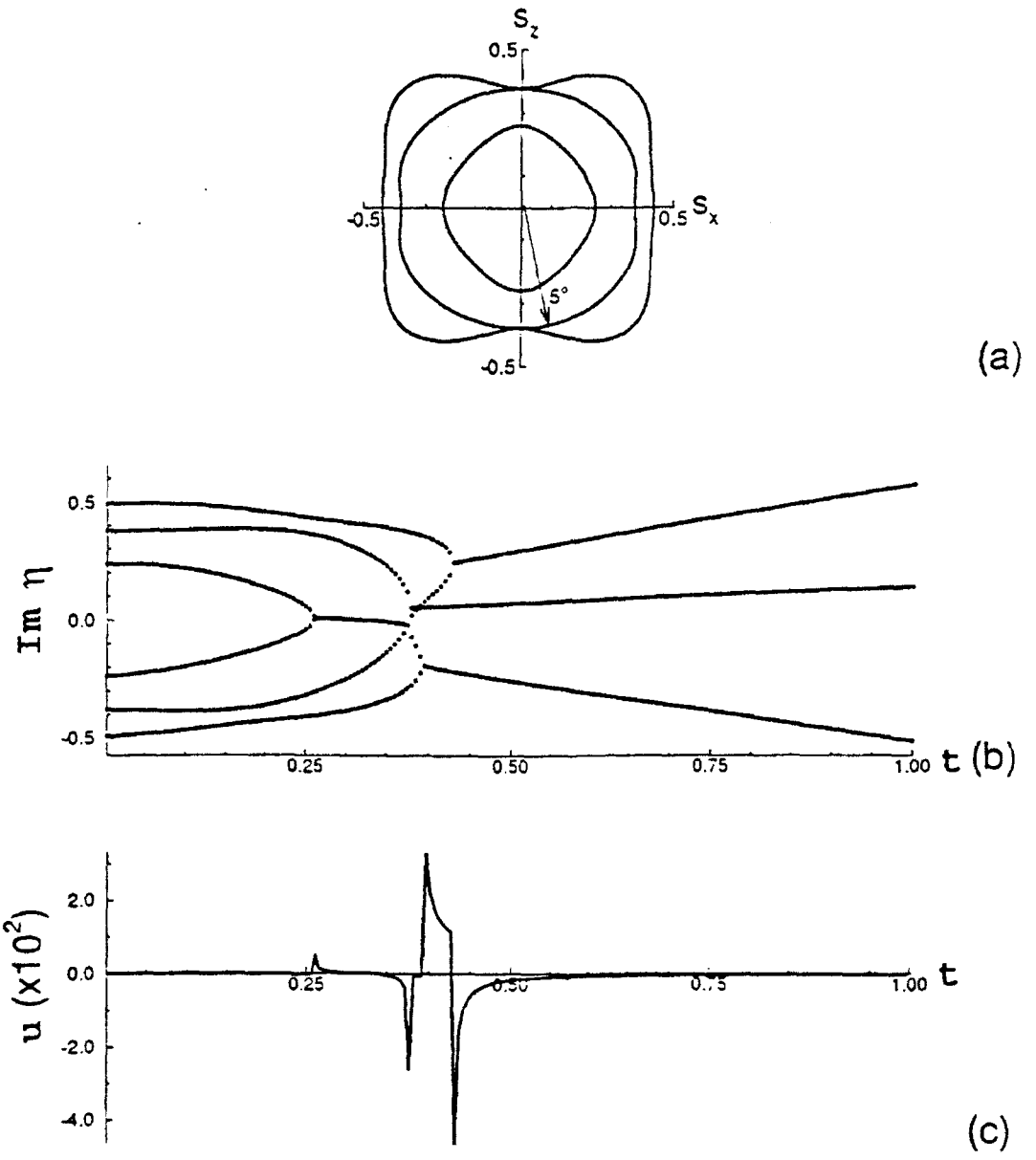

Figure 2.3: Various responses due to a line load in the infinite cubic medium of InAs ($\phi = 30°$) : (a) Wave propagation direction (5°) on the slowness surface ; (b) Imaginary part of η variation versus time (microsec) ; (c) Horizontal displacement u versus time (microsec) along $\theta = 5°$

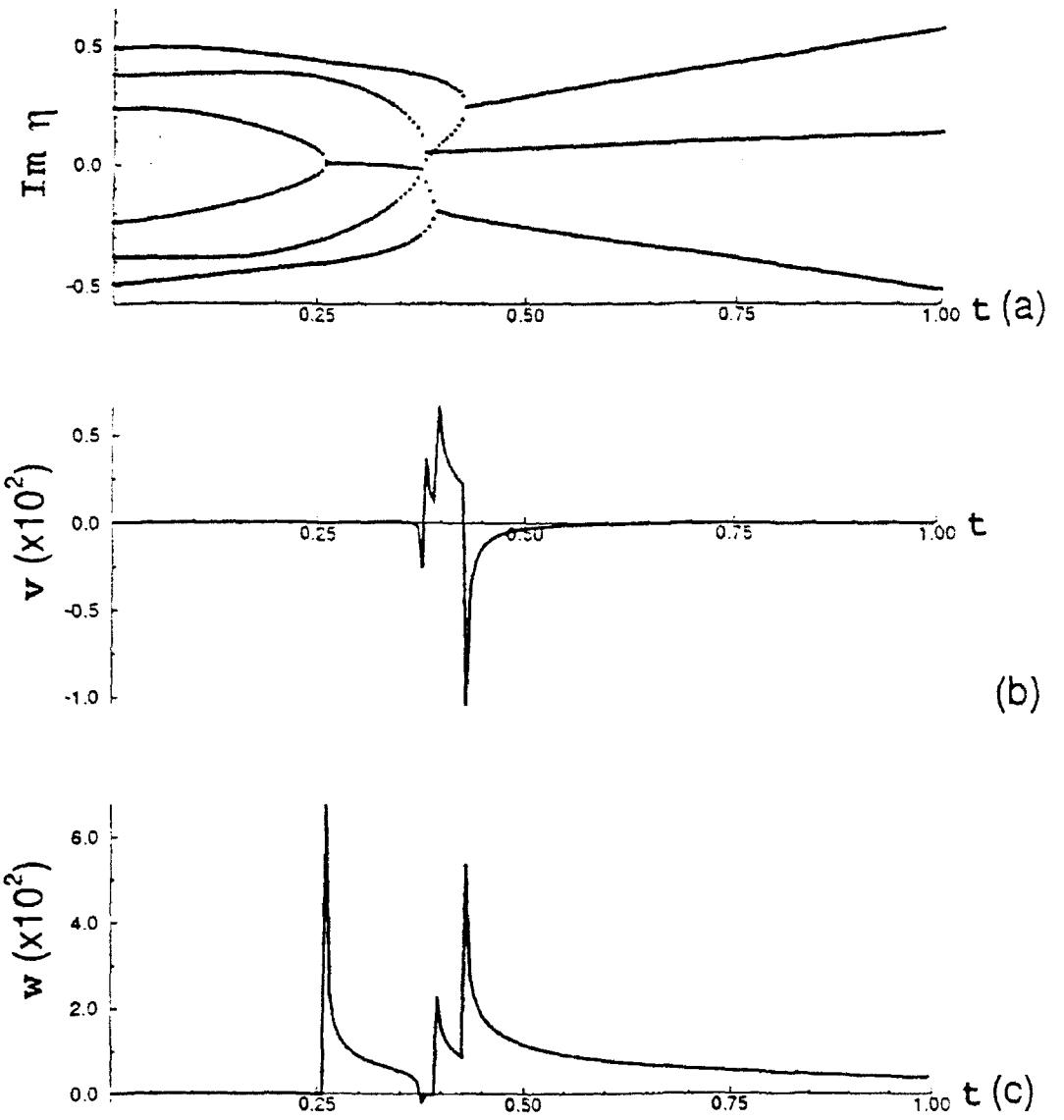

Figure 2.4: Various responses due to a line load in the infinite cubic medium of InAs ($\phi = 30°$) : (a) Imaginary part of η variation versus time (microsec) ; (b) Transverse displacement w versus time (microsec) along $\theta = 5°$; (c) Vertical displacement w versus time (microsec) along $\theta = 5°$

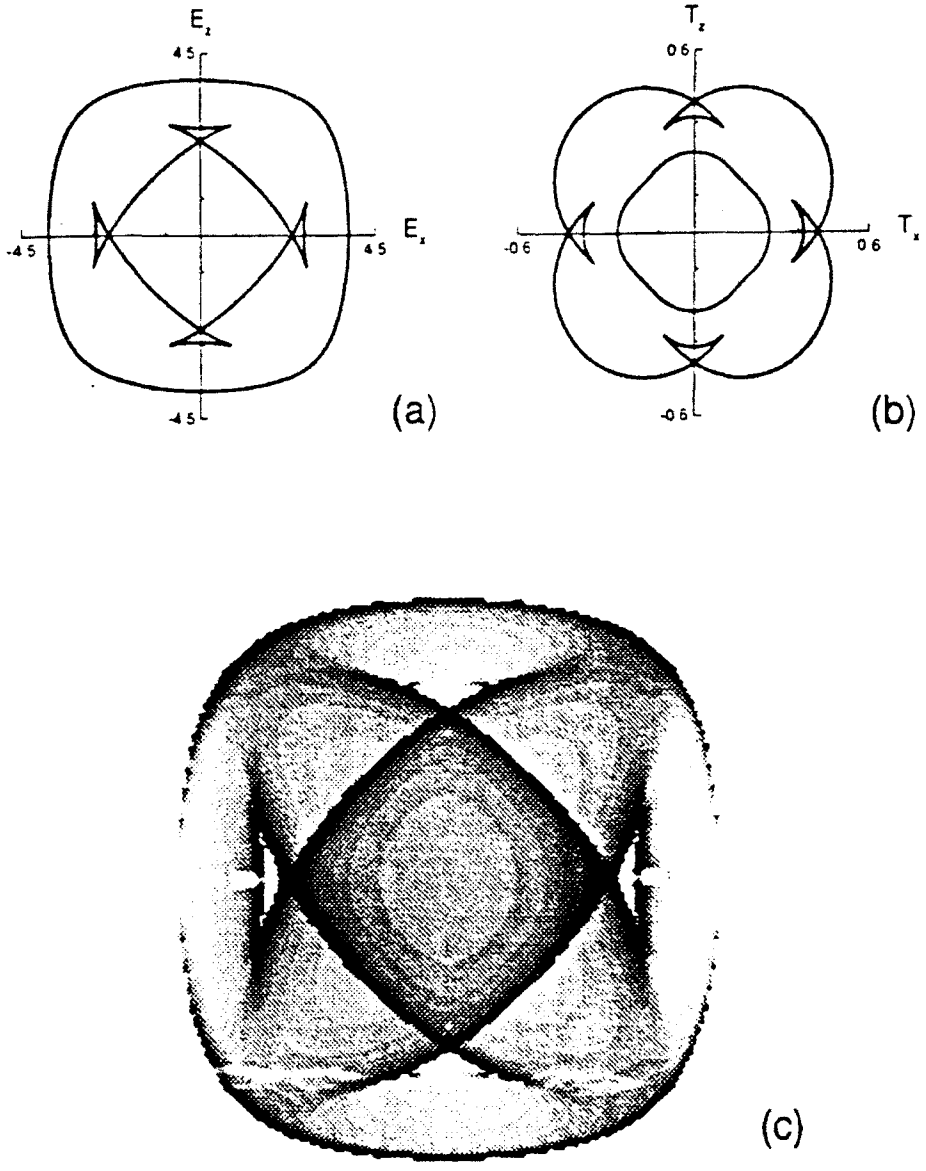

Figure 2.5: Displacement field due to a line load in the infinite cubic medium of InAs ($\phi = 0°$) : (a) Slowness surface ; (b) Energy slowness ; (c) Energy flow ; (d) Snap shot of displacement field at t=0.2 microsec

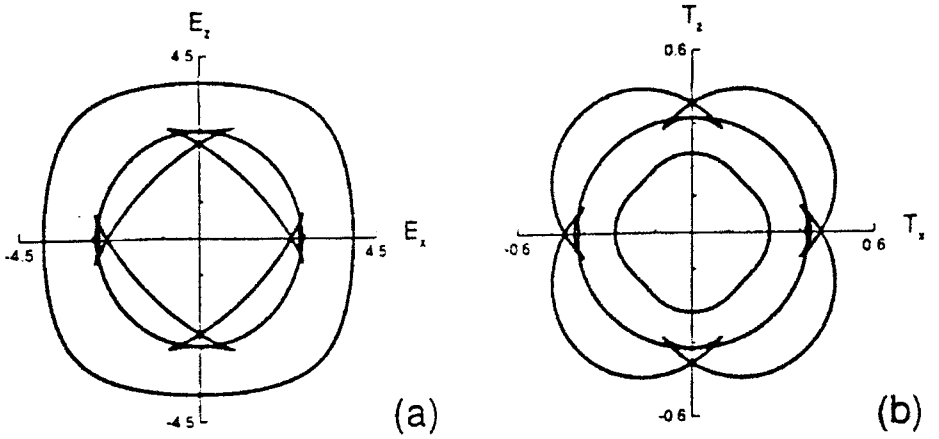

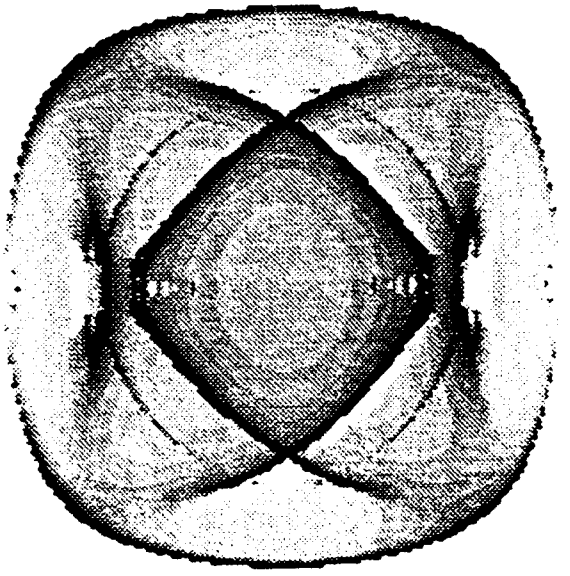

Figure 2.6: Displacement field due to a line load in the infinite cubic medium of InAs (ϕ = 10°) : (a) Slowness surface ; (b) Energy slowness ; (c) Energy flow ; (d) Snap shot of displacement field at t=0.2 microsec

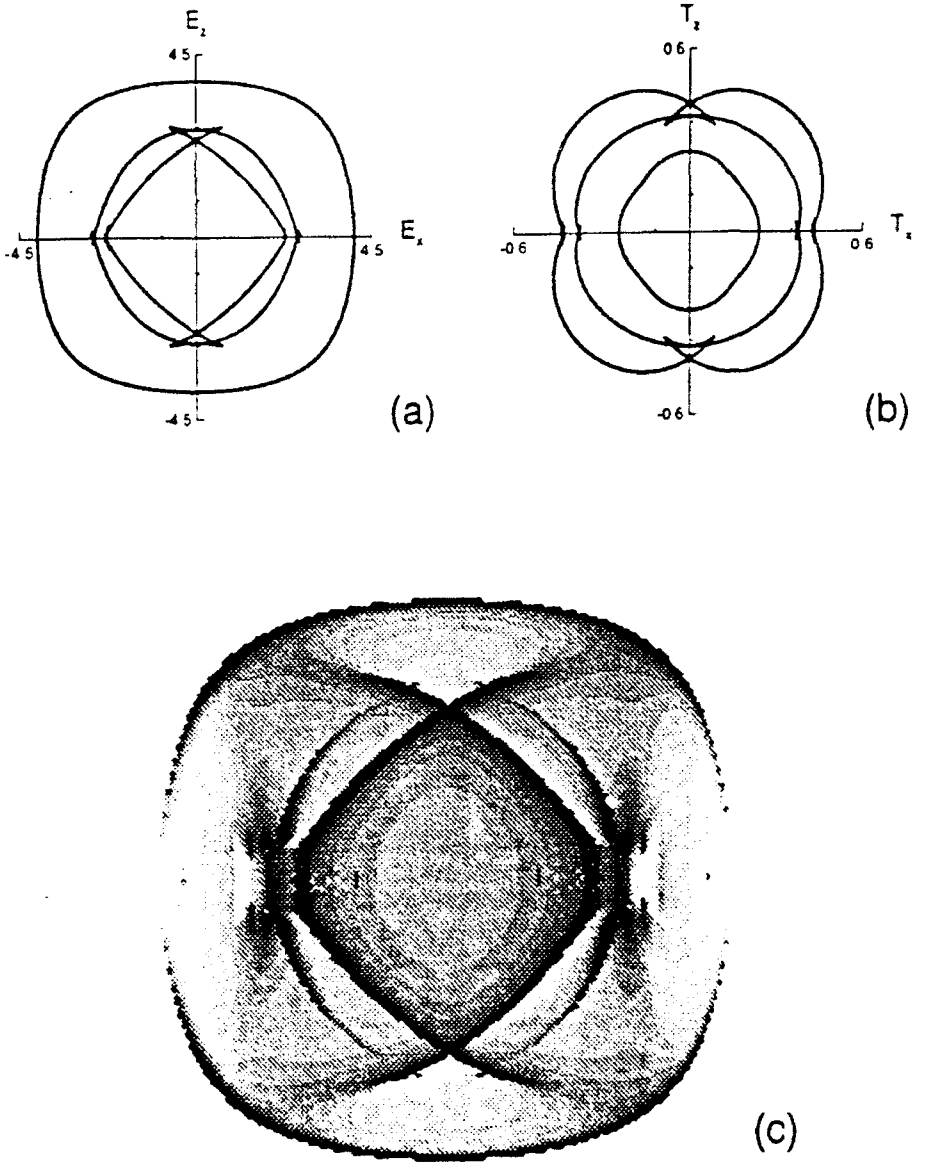

Figure 2.7: Displacement field due to a line load in the infinite cubic medium of InAs ($\phi = 20°$) : (a) Slowness surface ; (b) Energy slowness ; (c) Energy flow ; (d) Snap shot of displacement field at t=0.2 microsec

0.0, 0.2)(mm). Sharp variations of displacements are due to the arrival of the various waves. As time increases, the displacements approach to zero, which is consequence of the direc delta function. The results in figure 9 are as expected physically. A strong peak is observed that shows the existence of a surface or a Rayleigh wave. We can clearly recognize quasi-longitudinal wave, 2 quasi-shear waves, and a surface wave.

The second case is to numerically calculate the response generated by the line load on the surface. The surface is free from tractions except the line load along the x_2-axis. Many researchers (Taylor, Krout, etc) investigated this problem for the various line load such as direc delta function or heavyside step function with respect to time. Analytical results for the heavyside step function surface line load in the half-space media are given in [29]. We present numerical illustrations of the snap shot for the displacement fields generated by direc delta line load. Figure 10 present snap shots of radical displacement field at fixed time ($t = 0.2$) for isotropic steel (a), perturbed steel of $\phi = 0°$ (b), and perturbed steel of $\phi = 30°$ (c). A spatial grid of 100x100 points are generated for the first quadrant. The fourth quadrant is then generated by the mirror of the first quadrant. The color scheme runs from white (maximum) to black (minimum). In these pictures we can clearly recognize the wave curves (head wave, surface wave, and three bulk wave forms). The surface wave attribution is shown at inside of longitudinal wave front and near to the horizontal plane surface.

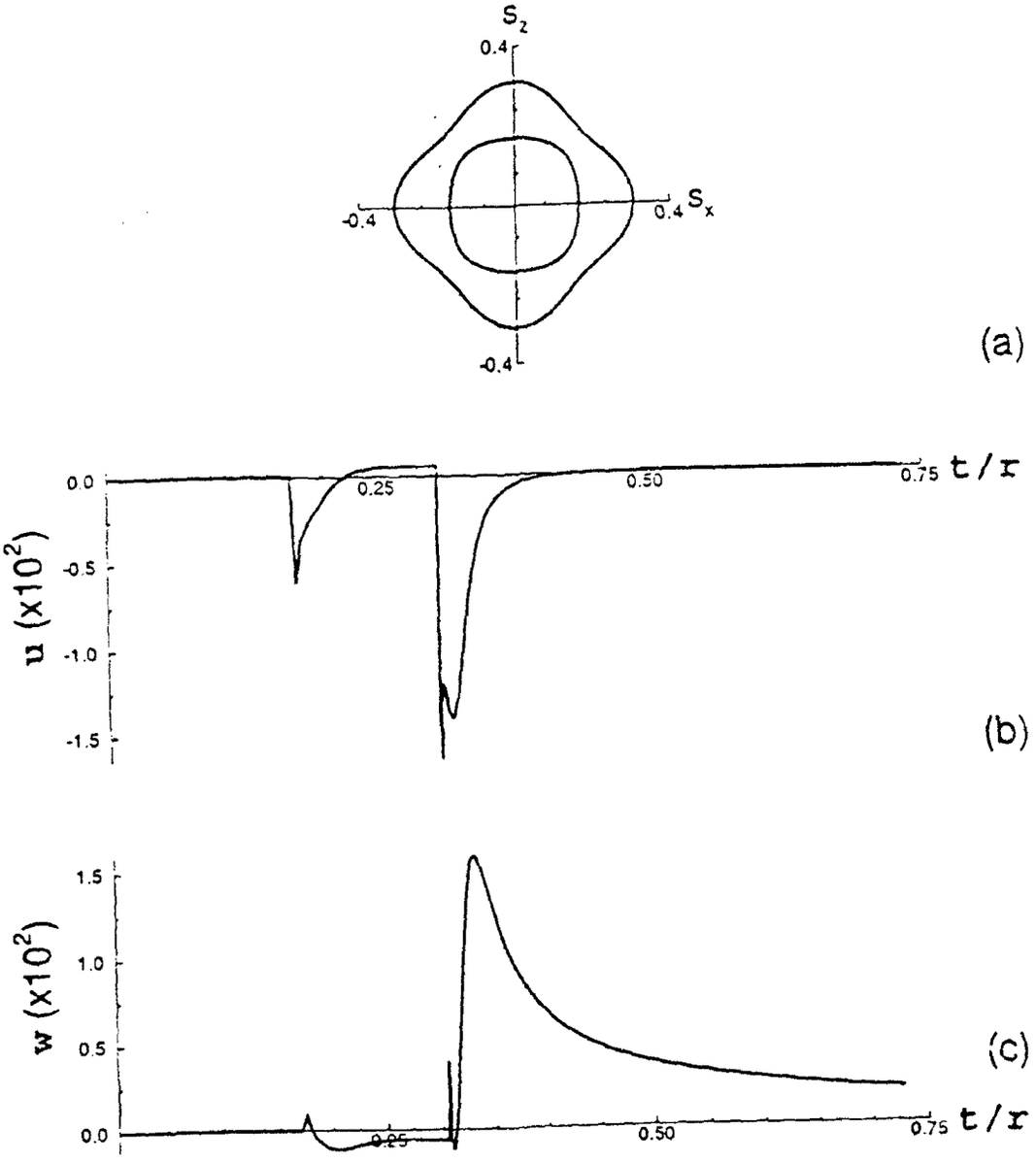

Figure 2.8: Displacements on the surface due to an internal line load in the semi-infinite cubic medium of perturbed steel (f=1.5, $\phi = 0°$), r/d = 5 : (a) Slowness surface ; (b) Horizontal displacement u versus t/r ; (b) Vertical displacement w versus t/r

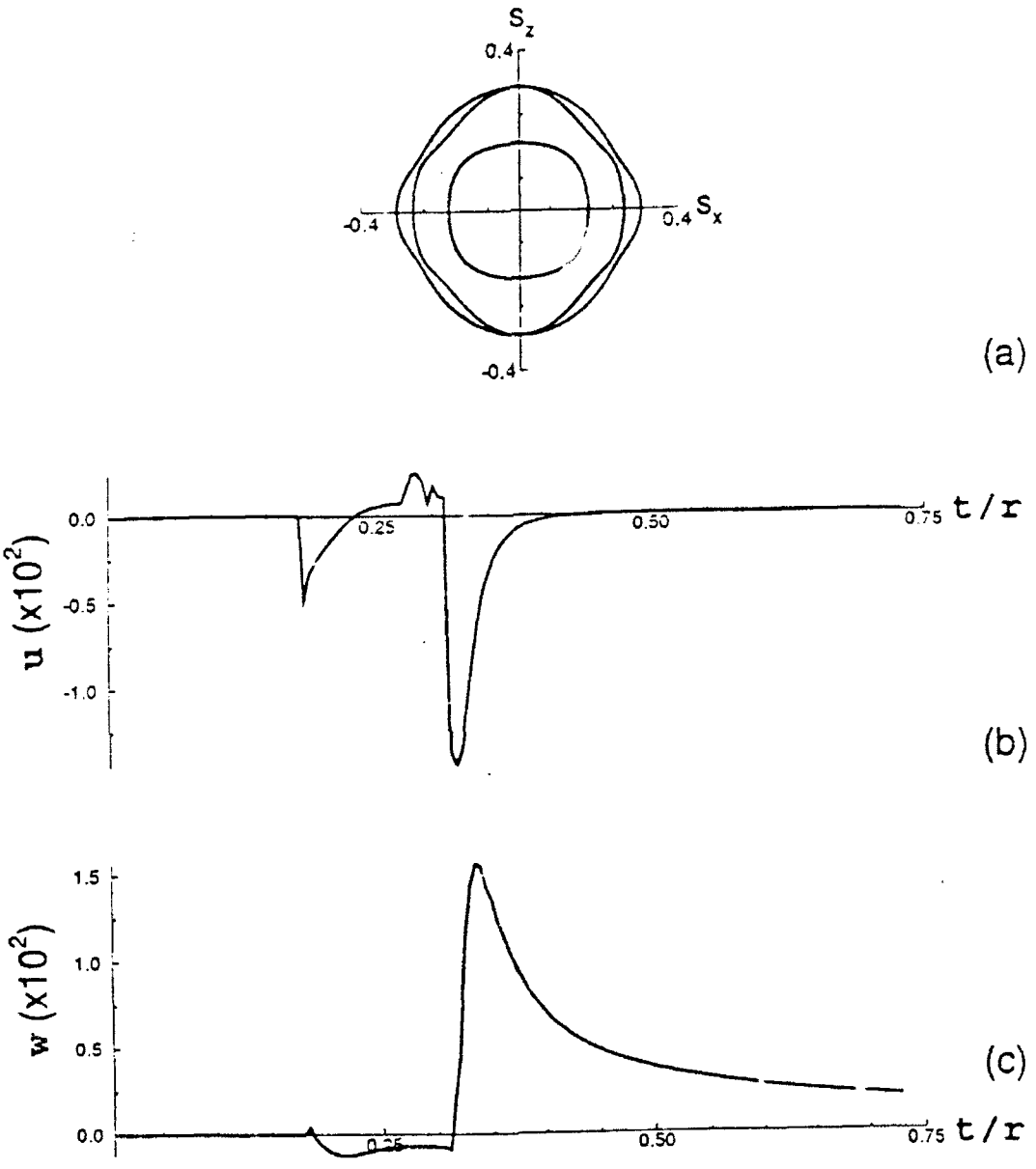

Figure 2.9: Displacements on the surface due to an internal line load in the semi-infinite cubic medium of perturbed steel (f=1.5, ϕ = 30°), r/d = 5 : (a) Slowness surface ; (b) Horizontal displacement u versus t/r ; (b) Vertical displacement w versus t/r

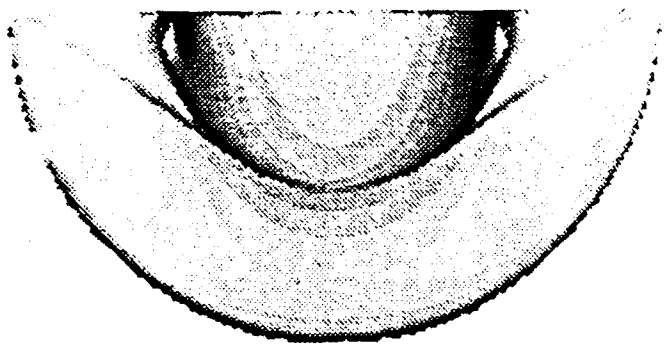

(a)

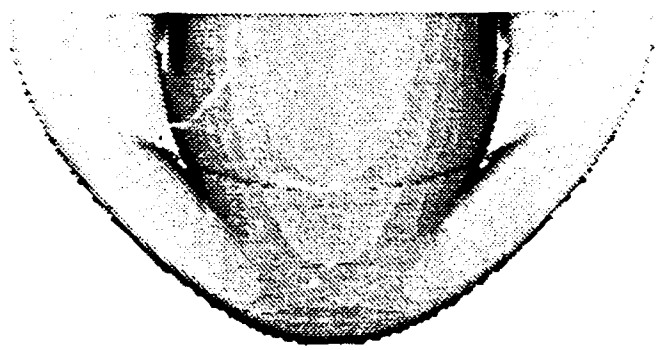

(b)

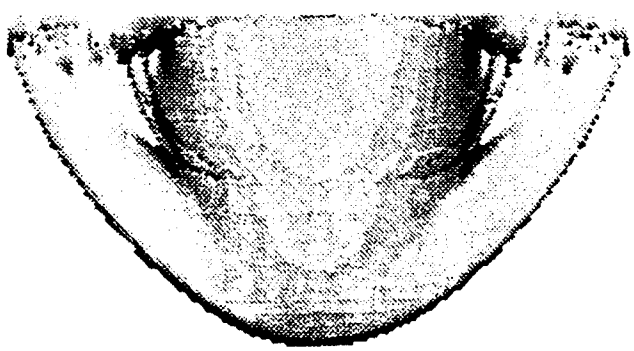

(c)

Figure 2.10: Snap shot of displacement field due to a surface line load of the semi- infinite medium at t=0.2 microsec : (a) Displacement field for steel ; (b) Displacement field for perturbed steel (f=1.5, $\phi = 0°$) ; (c) Displacement field for perturbed steel (f=1.5, $\phi = 30°$)

Bibliography

[1] A. H. Nayfeh, "The General Problem of Elastic Wave Propagation in Multilayered Anisotropic Media", Journal of the Acostical Society of America. 89, 4,1521- 1531, 1991.

[2] D. E. Chimenti and A. H. Nayfeh, "Ultrasonic Reflection and Guided Waves in Fluid-Coupled Composite Laminates", J. Nondestructive Evaluation, Vol. 9, No. 2/3, (1990)

[3] A. H. Nayfeh and D. E. Chimenti, "Free Wave Propagation in Plates of General Anisotropic Media," J. Appl. Mech., Vol.55, 863-870(1989).

[4] A. H. Nayfeh and D. E. Chimenti, "Ultrasonic Wave Reflection from Liquid-Coupled Orthotropic Plates with Application to Fibrous Composites," J. Appl. Mech., Vol.55, 863-870(1988).

[5] A. H. Nayfeh and D. E. Chimenti, "Propagation of Guided Waves in Fluid-Coupled Plates of Fiber-Reinforced Composites," J. Appl. Mech., Vol.83, pp1736(1988).

[6] D. E. Chimenti and A. H. Nayfeh, "Ultrasonic leaky waves in a solid plate separating fluid and vacuum media," J. Acous. Soc. Am, Vol.85(2), 1989

[7] J. L. Synge, "Elastic waves in anisotropic Media", J. Math. Phys., Vol.35, 323-334(1957)

[8] F. I. Fedorov, "Theory of Elastic Waves in Crystals, Plenum, New York, (1968).

[9] M. I. P. Musgrave, "Crystal Acoustics", Holden Day, San Francisco, (1970).

[10] Lord Rayleigh, "On the free vibrations of an infinite plate of homogeneous isotropic elastic materual, Proc. London Mathematical Society, 20, 225 (1889)

[11] H.Lamb, "On the Propagation of Tremors Over the Surface of an Elastic solid", Phil. Trans. Roy. Soc.,London, ser.A, Vol.203, 1-42(1904).

[12] H.Lamb, "On Waves in an Elastic Plate", Phil. Trans. Roy. Soc., London, Ser.A, Vol.93, 114-128(1917)

[13] E. R. Lapwood, "The Disturbance due to a Line Source in a Semi-infinite Elastic Medium", Phil. Trans. Roy. Soc., London, Ser.A, Vol.242, 9-100(1949).

[14] G. Eason, J.Fulton and I. N. Sneddon, "The Generation of Wave in an Infinite Elastic Solid by Variable Body Forces",Phil. Trans. Roy. Soc.,London, Ser.A, Vol.248, 575-308(1956).

[15] C. Pekeris and H. Lifson, "Motion of the Surface of a Uniform Elastic Half-Space Produced by a Buried Pulse", J. Acous. Soc. Am., Vol.29, 1233-1238(1957).

[16] L. Cagniard, "Reflection and Refraction of Progressive Seismic Waves" (trans. by E. Flinn and C. Dix. McGraw-Hill, New York, 1962)

[17] W. W. Garvin, "Exact Transient Solution of the Beried Lmne Source Problem", Proc. Roy. Soc., London, Ser.A, Vol.234, 528-541(1956).

[18] A. T. De Hoop, "A Modification of Cagniard's Method for Solving Seismic Pulse Problems", Appli. sci. Res., B, Vol.8, 349-357(1960).

[19] M. Shmuely, "Response of Plates to Transient Source", J. of Sound and Vibration, Vol.32(4), 507-512(1974)

[20] M. Shmuely, "Stress Wave Propagation in Plates Subjected to a Transient Line Source", Int. J. Solid Structure, Vol.11, 679-691(1975)

[21] Y. H. Pao, R. R. Gajewski and A. N. Ceranoglu,"Acoustic Emission and Transient Waves in an Elastic Plate", J. Acoust. Soc. Am., Vol.65(1), 96-105(1979)

[22] E. A. Kraut, "Advances in the Theory of Anisotropic Elastic Wave Propagation", Rev. of Geophysics, Vol.1, No.3, 401-448(1963).

[23] R. Burridge, "Lamb's Problem for an Anisotropic Half-Space", Quart. J. Mech. and Applied Math., Vol.23, 81-98(1971).

[24] R. Burridge, "The Directions in which Rayleigh Waves may be Propagated on Crystals", Quart. J. Mech. and Applied Math., Vol.23, 217-224(1979).

[25] J. H. Woodhouse, "Surface Waves in a Laterally Varying Layered Structure", Geophysics. J. R. astr. Soc, Vol.37, 461-490(1974). ffi

[26] G. J. Fryer and L. N. Frazer, "Seismic Waves in stratified anisotropic media," Geophysics. J. R. astr. Soc., Vol.78, 691-710(1984)

[27] G. J. Fryer and L. N. Frazer, "Seismic Waves in stratified anisotropic media-2 Elastodynamic Eigensolutions for some Anisotropic System", Geophysics. J. R. astr. Soc., Vol.91, 73-101(1987)

[28] J. H. M. T. Van Der Hijden, "Radiation from an Impulsive Line Source in an Unbounded Homogeneous Anisotropic Medium", Geophysics. J. R. astr. Soc., Vol.91, 355-372(1987).

[29] T. Taylor, "Transient Elastic Waves on Anisotropic Half-spaces", Ph.D. Dissertation, University of Cincinnati, 1989

[30] W. Ewing, W.Jardetzky and F. Press, Elastic Waves in Layered Media. (McGrraw Hill, New york, 1957)

[31] J. P. Achenbach, Wave Propagations in Elastic Solids, (American Elservier Pub. Co., New York, 1973)

[32] Y. C. Fung, Foundation of Solid Mechanics, (Prentice-Hall, Englewood Cliffs, N. J. 1965)

Appendix A

Various coefficients of characteristic eq.(18) are given by

$$\begin{aligned}
\Lambda_{11} &= c_{55}\alpha^2 - c_{11}\eta^2 - \rho \\
\Lambda_{12} &= c_{45}\alpha^2 - c_{16}\eta^2 \\
\Lambda_{13} &= -j\eta\alpha(c_{13} + c_{55}) \\
\Lambda_{22} &= c_{44}\alpha^2 - c_{66}\eta^2 - \rho \\
\Lambda_{23} &= -j\eta\alpha(c_{36} + c_{45}) \\
\Lambda_{33} &= c_{33}\alpha^2 - c_{55}\eta^2 - \rho
\end{aligned} \tag{2.55}$$

$$
\begin{aligned}
A_1 &= D_1 \\
A_2 &= D_2\eta^2 + D_3\rho \\
A_3 &= D_4\eta^4 + D_5\rho\eta^2 + D_6\rho^2 \\
A_4 &= D_7\eta^6 + D_8\rho\eta^4 + D_9\rho^2\eta^2 + \rho^3
\end{aligned} \tag{2.56}
$$

Appendix B

Various coefficients of polynomial for Cargniard-DeHoop contour are given by

$$
\begin{aligned}
B_6 &= D_2x_3^2x_1^4 - D_4x_3^4x_1^2 - D_1x_1^6 + D_7x_3^6 \\
B_5 &= C_1jt \\
B_4 &= C_2t^2 + D_3x_3^2x_1^4 - D_5x_3^4x_1^2 + D_8x_3^6 \\
B_3 &= C_3jt^3 + C_4jt \\
B_2 &= C_5t^4 + C_6t^2 - D_6x_3^4x_1^2 + D_9x_3^6 \\
B_1 &= 6D_1jx_1t^5 + 4D_3jx_3^2x_1t^3 + 2D_6x_3^4x_1t \\
B_0 &= D_1t^6 + D_3x_3^4t^4 + D_6x_3^4 + \rho^3x_3^6
\end{aligned} \tag{2.57}
$$

$$
\begin{aligned}
C_1 &= 6D_1x_1^5 + 2D_4x_3^4x_1 - 4D_2x_3^2x_1^3 \\
C_2 &= 15D_1x_1^4 - 6D_2x_3^2x_1^2 + D_4x_3^4 \\
C_3 &= 4D_2x_3^2x_1 - 20D_1x_1^3 \\
C_4 &= -4D_3x_3^2x_1^3 + 2D_5x_3^4x_1 \\
C_5 &= D_2x_3^2 - 15D_1x_1^2 \\
C_6 &= -6D_3x_3^2x_1^2 + D_5x_3^4
\end{aligned} \tag{2.58}
$$

$$
\begin{aligned}
D_1 &= c_{33}c_{45}^2 - c_{33}c_{44}c_{55} \\
D_2 &= c_{11}c_{33}c_{44} + c_{55}F_1 - c_{16}c_{33}c_{45} - c_{45}F_2 + (c_{13} + c_{55})F_3 \\
D_3 &= [c_{55}(c_{33} + c_{44}) + c_{33}c_{44} - c_{45}^2]\rho \\
D_4 &= [(c_{13} + c_{55})F_4 + c_{45}c_{16}c_{55} + c_{16}F_2 - c_{55}^2c_{66} - c_{11}F_1] \\
D_5 &= [(c_{13} + c_{55})^2 + 2c_{45}c_{16} - F_1 - c_{55}(c_{55} + c_{66}) - c_{11}(c_{33} + c_{44})]\rho
\end{aligned}
$$

$$
\begin{aligned}
D_6 &= -(c_{33}+c_{44}+c_{55})\rho^2 \\
D_7 &= (c_{11}c_{55}c_{66}-c_{16}^2c_{55}) \\
D_8 &= [c_{11}(c_{55}+c_{66}-c_{16}^2]\rho \\
D_9 &= (c_{11}+c_{55}+c_{66})\rho^2
\end{aligned} \tag{2.59}
$$

$$
\begin{aligned}
F_1 &= c_{33}c_{66}+c_{44}c_{55}-(c_{36}+c_{45})^2 \\
F_2 &= c_{33}c_{16}+c_{45}c_{55}-(c_{36}+c_{45})(c_{13}+c_{55}) \\
F_3 &= c_{45}(c_{36}+c_{45})-c_{44}(c_{13}+c_{55}) \\
F_4 &= c_{66}(c_{13}+c_{55})-c_{16}(c_{36}+c_{45})
\end{aligned} \tag{2.60}
$$

Appendix C

Various coefficients of polynomial for Cargniard-DeHoop contour are given by

$$
\begin{aligned}
G_{11} &= D_{23}D_{35}-D_{33}D_{25} \\
G_{12} &= D_{33}D_{15}-D_{13}D_{35} \\
G_{13} &= D_{13}D_{25}-D_{15}D_{23} \\
G_{21} &= D_{31}D_{25}-D_{21}D_{35} \\
G_{22} &= D_{11}D_{35}-D_{31}D_{15} \\
G_{23} &= D_{15}D_{21}-D_{11}D_{25} \\
G_{31} &= D_{21}D_{33}-D_{31}D_{23} \\
G_{32} &= D_{31}D_{13}-D_{11}D_{33} \\
G_{33} &= D_{11}D_{23}-D_{13}D_{21}
\end{aligned} \tag{2.61}
$$